WILLIAM & MARY
CHARTERED 1693

Reports

12-1-2011

Assessment of Oyster Reefs in Lynnhaven River as a Chesapeake Bay TMDL Best Management Practice

Mac Sisson
Virginia Institute of Marine Science

M. Lisa Kellogg
Virginia Institute of Marine Science

Mark Luckenbach
College of William and Mary
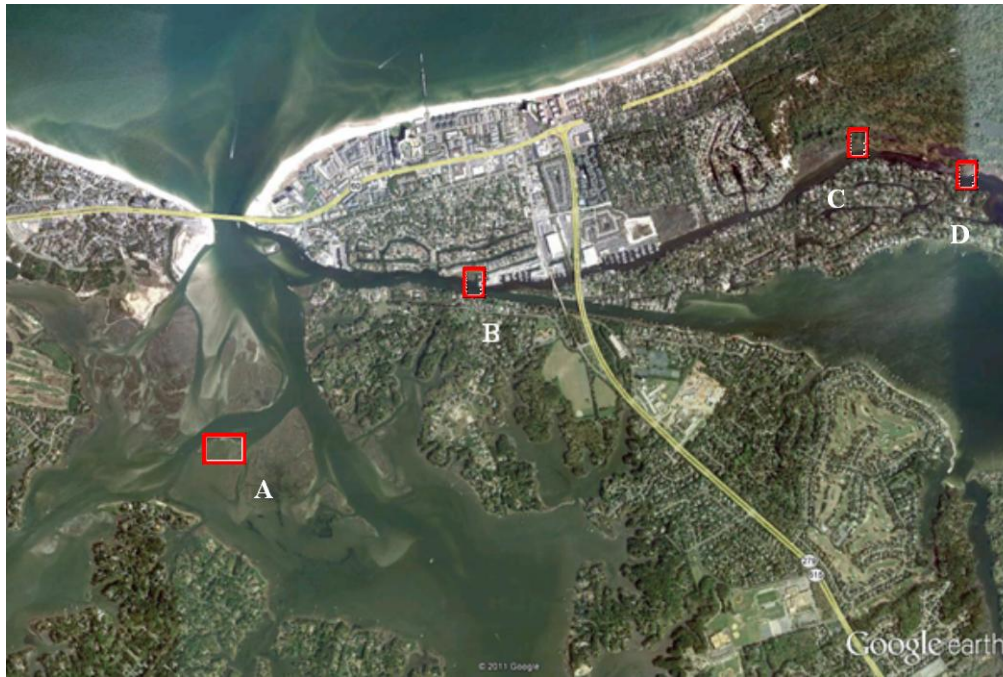
Rom Lipcius
VIMS

Follow this and additional works at: https://scholarworks.wm.edu/reports

Part of the Marine Biology Commons

ASSESSMENT OF OYSTER REEFS IN LYNNHAVEN RIVER AS A CHESAPEAKE BAY TMDL BEST MANAGEMENT PRACTICE

Mac Sisson, Lisa Kellogg, Mark Luckenbach, Rom Lipcius,
Allison Colden, Jeff Cornwell, and Michael Owens

Final Report to the

U. S. Army Corps of Engineers, Norfolk District
and
The City of Virginia Beach

Special Report No. 429
In Applied Marine Science and Ocean Engineering

Virginia Institute of Marine Science
Department of Physical Sciences
Gloucester Point, Virginia 23062

December 2011

EXECUTIVE SUMMARY

1. The Norfolk District of the US Army Corps of Engineers and the City of Virginia Beach are working together on a cost-shared basis to evaluate the potential of using oyster reefs as a Chesapeake Bay Total Maximum Daily Load (TMDL) Best Management Practice.

2. In previous investigations, it has been found that oysters modify biogeochemical cycles by filtering large quantities of organic matter from the water column. The majority of this organic matter is either used directly by the oysters for growth and maintenance or deposited by oysters on the sediment surface where it becomes a source of food for an abundant and diverse community of organisms. The goals of this project were to estimate biomass-specific rates of filtration, biodeposition, nutrient sequestration and denitrification associated with intertidal and shallow subtidal reefs in the Lynnhaven River, VA.

3. Filtration rate and biodeposition rate were examined by re-analysis and statistical modeling of previously published data, and a selective synthesis of recent studies. In the re-analysis of previously published data, we found statistical problems with prior analyses. Our new analysis demonstrates that biodeposition rate and biofiltration rate are related in a positive and non-linear fashion to seston concentration in the water column and water temperature. In addition, biodeposition and biofiltration are positively related to oyster biomass (dry weight), such that water quality measures need not account for oyster reef height, but only oyster biomass as determined from oyster reef and habitat surveys.

4. We measured denitrification rates and standing stock nitrogen and phosphorus sequestration in relation to oyster density, bottom type, and tidal height at eight locations in the Lynnhaven River. At Humes Marsh, we measured these values on four oyster reefs that varied in oyster density and bottom type and one control site without oysters; in Long Creek measurements were made on three reefs that varied in oyster density, bottom type and tidal height.

Total nitrogen flux was positively related to oyster density at seven of eight locations within the Lynnhaven that we studied, indicating that oysters play an important role in depositing nitrogen on the bottom in this system. The majority of this nitrogen is recycled back into the water column as ammonium, nitrate, and nitrite; however, a significant amount is converted to di-nitrogen gas that then diffuses into the atmosphere. Nitrogen removal via denitrification at oyster reefs sites, comprised of a shell base and live oysters, ranged from 15.13 to 20.21 lbs. acre^{-1} month^{-1} compared to 1.03 lbs. acre^{-1} month^{-1} at a bare sediment site. Nitrogen sequestration in the tissues of oysters and other reef organisms ranged from 495.79 to 656.48 lbs. acre^{-1} on the reef sites compared to 32.6 lbs. acre^{-1} at a bare sediment site.

Our study clearly demonstrates that oyster reef restoration can improve water quality both by sequestering nitrogen in the tissues and shells of organisms and by converting organic nitrogen to nitrogen gas that is removed from the water column via diffusion back to the atmosphere, and by depositing TSS within the reef matrix.

5. Over the period 2005-2008, VIMS completed the successful development of an integrated numerical modeling framework for the Lynnhaven River system. This framework combines a high-resolution 3D hydrodynamic model (UnTRIM) that provides the required transport for a water quality model (CE-QUAL-ICM) that, in turn, provides intra-tidal predictions of 23 water quality state variables. The hydrodynamic model underwent an extensive calibration for surface elevation, salinity, and temperature and the water quality model was calibrated for dissolved oxygen, chl-a, various forms of nitrogen and phosphorus, and total suspended solids. Enhancements to these models to incorporate oyster reef dynamics are underway.

6. With respect to phosphorus, this investigation showed that there was no significant reduction from the water column due to the presence of oyster reefs in the Lynnhaven based on measurements of soluble reactive phosphorus flux measured under light and dark conditions.

7. Regarding the removal of sediment from the water column due to oyster reefs, the amount removed is controlled in large part by hydrodynamic advection, oyster biomass, seston concentration, and water temperature. Determinations of the amounts removed can be achieved through integration of the listed equations or more precisely through numerical modeling that integrates the equations with hydrodynamic models.

Findings or recommendations contained herein do not constitute Corps of Engineers approval of any project(s) or eliminate the need to follow normal regulatory permitting processes.

ACKNOWLEDGEMENTS

TABLE OF CONTENTS

LIST OF TABLES

LIST OF FIGURES

CHAPTER I. INTRODUCTION

The Lynnhaven River includes the Eastern Branch, Western Branch, Long Creek, Broad Bay, Crystal Lake, Linkhorn Bay and all of the tributaries. A great deal of effort has been extended by the City of Virginia Beach and the US Army Corps of Engineers (Norfolk District) towards restoring and protecting the Lynnhaven River. These agencies signed a feasibility cost-sharing agreement and embarked on determining suitable and acceptable means for designing and implementing the environmental restoration of the Lynnhaven.

Restoration planning for the Lynnhaven involved discussions with personnel from VIMS and URS Corporation of Virginia Beach, and it was soon resolved that a fully comprehensive system, including spatially high-resolution numerical modeling and watershed loading estimation, was required in order to address the water quality issues cited in the reconnaissance report and to provide the management option of a control strategy of attaining the required endpoints for environmental restoration.

Over the period 2005-2008, the ACE (Norfolk District) and the City of Virginia Beach contracted with VIMS for the development of hydrodynamic and water quality models for the Lynnhaven receiving waters and with URS Corporation for an adapted version of its HSPF (Hydrological Simulation Program – FORTRAN) watershed model to provide both freshwater flows and nutrient and sediment loadings from the Lynnhaven River Watershed for this region.

In early 2011, representatives of the City of Virginia Beach posed questions about the possible role of oyster reefs in the removal of both nutrients and sediments from the overlying water column and the feasibility of expanding oyster reef acreage in the Lynnhaven to meet future loading reductions required of the City of Virginia Beach by the upcoming Chesapeake Bay Total Maximum Daily Load (TMDL) mandates.

In August 2011, the ACE (Norfolk District) and the City of Virginia Beach contracted with VIMS to assess the Lynnhaven oyster reefs as a Chesapeake Bay TMDL Best Management Practice. Estimates of nutrient removal rates per acre as well as sequestration amounts per area would later provide the necessary water quality model input to assess water quality improvements resulting from the development of additional oyster reef acreages.

This report provides the results of VIMS efforts to assess nitrogen removal and sequestration capacity of nitrogen and phosphorus, as well as sediment removal, due to existing oyster reefs in the Lynnhaven River. Kellogg et al. (2011) assessed nutrient removal and sequestration capacity for restored and non-restored reefs in the Choptank River. Their study reported that, for a dense population (131 oysters m^{-2}), potential removal exceeding 540 lbs N acre-1 yr^{-1} as well as sequestrations of 871 lbs N $acre^{-1}$ and 139 lbs P $acre^{-1}$ occurred. For the Lynnhaven, efforts were made to span a range of oyster densities in the assessment of nutrient removal rates and sequestration quantities.

Inputs of nutrients and sediments to Chesapeake Bay and its tributaries have increased over time, leading to reduced water quality. Excess nutrient inputs enhance phytoplankton

production and can lead to anoxic conditions in bottom waters. Excess sediment inputs can lead to habitat degradation either by direct impacts (e.g. burial) or indirect impacts (e.g. reduction of light reaching vegetated benthic habitats). In response to excess inputs, the U.S. Environmental Protection Agency has imposed guidelines towards nutrient reduction goals for point source discharges for nitrogen, phosphorus, and suspended sediments. As the Lynnhaven has approximately 1050 outfalls draining its watershed into the receiving waters of its three branches, the City of Virginia Beach is submitting its plan for nutrient and sediment reduction to the Virginia Department of Conservation Resources (DCR).

The burden of meeting these reduction targets falls largely upon local governments, which must look to a variety of options to reduce nutrient and sediment concentrations in the waters adjacent to their jurisdictions. The City of Virginia Beach is faced with making significant reductions in the nutrient and sediment concentrations in the Lynnhaven River. In addition to meeting these goals by reducing the loadings of nitrogen, phosphorus, and sediments into the Lynnhaven basin, the City is interested in evaluating the efficacy of using native oyster restoration as a means to remove nutrients and sediment from the water column.

It has long been recognized that, through their filtration activity, oysters have the capacity to affect water quality in Chesapeake Bay (Newell 1988) and other coastal waters (Dame et al. 1980). It is important to recognize, however, that filtration alone does not permanently remove nutrients or sediment from the aquatic environment. Sediments may be resuspended and nutrients undergo complex biogeochemical processes that ultimately determine their fate within the ecosystem. Figure I.1 shows a diagram of major nitrogen pathways in a water body with an oyster reef and without significant benthic micro- or macroalgal populations. Phytoplankton use dissolved inorganic nitrogen for their growth (A). Oysters and other reef associated organisms filter phytoplankton and other particulate organic matter from the water column (B). Some of the associated nitrogen is incorporated into the tissues of organisms and some is deposited on the surface of the sediments (C). Under the right conditions, the nitrogen in these biodeposits can be transformed through a series of microbial-mediated processes known as nitrification and denitrification into nitrogen gas (D) which diffuses out of the sediments and back to the atmosphere (E) where it is no longer available for phytoplankton growth (Newell et al. 2005). In the presence of significant benthic algal populations, these pathways are modified by competition between algae and microbes for nitrogen compounds which can reduce rates of nitrification and denitrification. Regardless of the specific pathways involved, the capacity of restored oyster reefs to alter nitrogen cycles and enhance denitrification rates is potentially one of the most valuable services these ecosystems can provide (Kellogg et al. 2011; Newell 2004; Newell et al. 2002, 2005; Piehler and Smyth 2011).
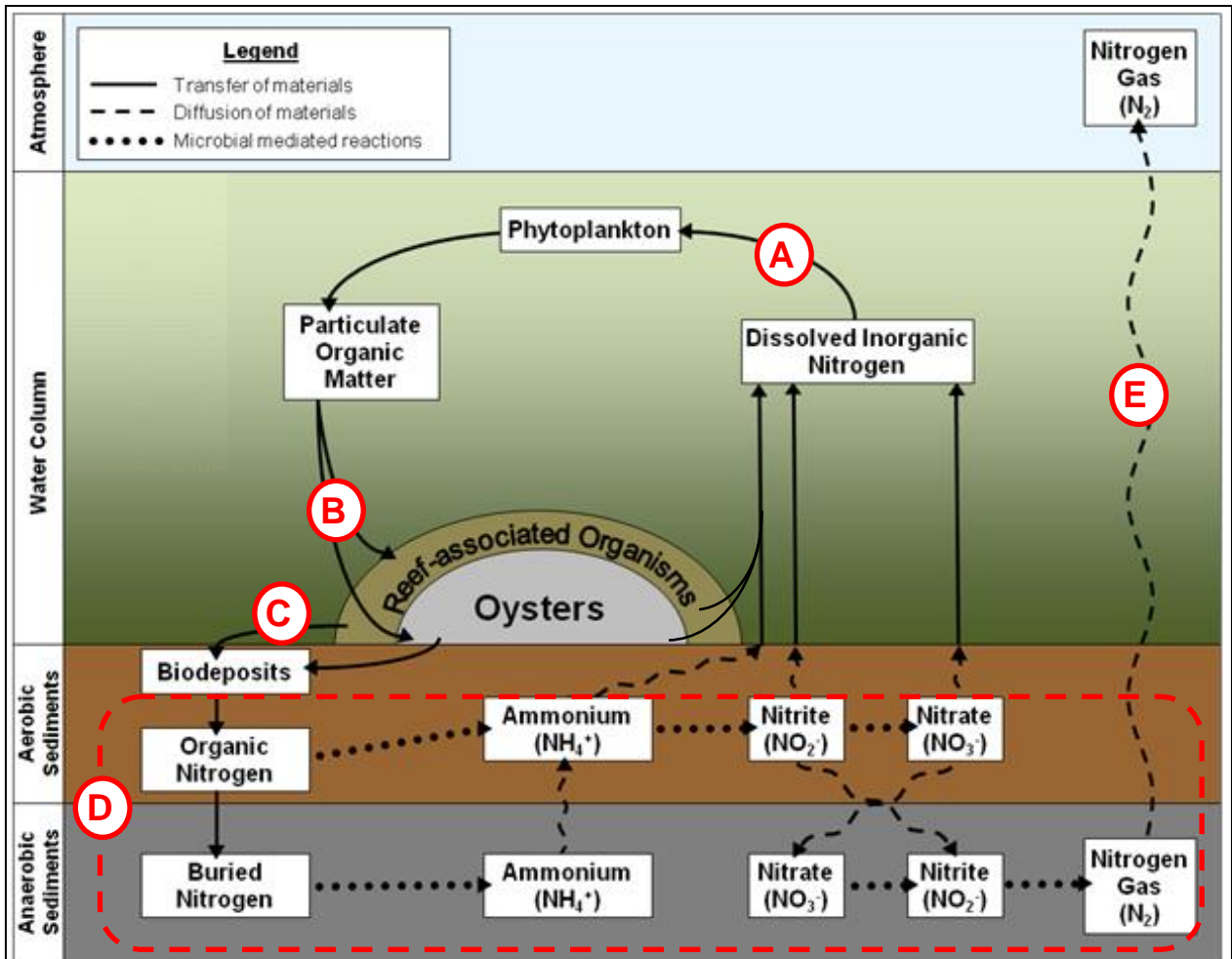
Figure I.1. Major nitrogen pathways on an oyster reef: phytoplankton use dissolved inorganic nitrogen for their growth (A), oysters and other reef associated organisms filter phytoplankton and other particulate organic matter from the water column (B), some of the associated nitrogen is incorporated into the tissues of the organisms and some is deposited on the surface of the sediments (C), and, given the right conditions, a portion of the nitrogen in these biodeposits is transformed into nitrogen gas (D) which diffuses out of the sediments back to the atmosphere (E) where it is no longer available to phytoplankton for growth (Diagram adapted from Newell et al. 2005).

Although oyster reef ecosystems are known to have significant impacts on biogeochemical cycles (e.g. Dame et al. 1989), direct measurement of biogeochemical fluxes is logistically difficult. Methods commonly used to measure biogeochemical fluxes in soft-sediment systems (e.g. collection and incubation of sediment cores) are impractical for use on oyster reefs for several reasons: 1) the physical structure of the reef does not allow core sampling without significant disturbance of the microbial community at the sediment-water interface, 2) the diameter of a single clump of oysters is often greater than the diameter of the core tubes typically used for these studies, and 3) the high respiration rates typical of oyster reefs can rapidly deplete oxygen during incubations. Past approaches to understanding the biogeochemical effects of oyster communities have included benthic tunnels in marsh creeks

(Dame et al. 1989), core incubations to simulate the effects of oyster biodeposits (Newell et al. 2002; Holyoke 2008), and incubations of sediment cores collected adjacent to oyster communities (Piehler and Smyth 2011). Recently, Kellogg et al. (2011) developed a technique for directly measuring fluxes of di-nitrogen from oyster reefs that combines inclusion of a realistic oyster reef benthic community with high precision measurements. This technique was successfully employed to measure denitrification on a subtidal restored oyster reef in Maryland.

Sequestration of nutrients in the tissues of reef organisms also represents a means of removing nitrogen and phosphorus from the water column (Higgins et al. 2011; Kellogg et al. 2011). The extent to which this mechanism of nutrient removal assists in achieving TMDLs will depend upon the length of time the nutrients are sequestered and/or the extent to which they are transported out of the system. In general, nutrient sequestration in the tissues of organisms only lasts as long as the soft tissues and hard structures they build as they grow remain intact. Nutrients sequestered in the soft tissues of an oyster could remain sequestered for years, whereas the nutrients sequestered in the tissues of an amphipod could last only a few weeks if that amphipod dies without being consumed by another organism. Nutrients sequestered in the calcium carbonate structures created by many organisms (e.g. the shells of oysters) have the potential to sequester nutrients for years to decades (Powell et al. 2006) and, if buried in sediments, centuries to millennia (Kirby et al. 1998). The fate of nutrients sequestered in the tissues of reef organisms consumed by predators will depend upon a variety of factors including the assimilation efficiency of the predator and its life history.

Oysters have the capacity through the deposition of feces and pseudofeces (collectively called *biodeposits*; C in Fig. I.1) to remove large amounts of suspended sediments, as well as organic matter, from the water column. Oyster reefs have been shown to enhance sedimentation rates via accumulation of biodeposits (Haven and Morales-Alamo 1972) and enhancement of sediment deposition (DeAlteris 1988). The topographically complex, three-dimensional reef structures created by oysters as they grow alter flow characteristics in the vicinity of the reef. The high density of roughness elements (i.e. oyster shells) creates both a layer of decreased flow within the reef and increased turbulence in the overlying water column. The increase in turbulence above the reef results in higher numbers of sediment particles entering the reef matrix than would fall upon a soft sediment surface (i.e. mud or sand). Once these particles enter the reef matrix, they encounter lower flow speeds that result in greater rates of deposition. Once these particles have reached the surface of the sediments within the reef matrix, resuspension rates are low because flow speeds and turbulence at the sediment water interface are low. Another mechanism that enhances sediment deposition and reduces resuspension on oyster reefs is feeding activities of oysters. The seston that oysters filter from the water column contains suspended sediment particles in addition to the phytoplankton and other organic particles that they ultimately consume. After sorting sediment and other undesirable particles from the seston, these particles are packed in mucus and deposited as pseudofeces. Because these particles are bound in mucus and now have a larger effective particle size, they are less likely to be resuspended (Haven and Morales-Alamo 1972).

To fully appreciate the role that oyster reefs can play in removing nutrients and sediments from the water column we need to determine the size of the pools (i.e., the size of the boxes

in Fig. I.1) and the rate of fluxes between boxes (the magnitude of the arrows in Fig. I.1) and we then need to incorporate these values into tributary-scale water quality models.

The 3D water quality model developed by VIMS for use in the Lynnhaven River is the US Army Corps of Engineers model CE-QUAL-ICM. This model was initially developed as one component of a model package employed to study eutrophication processes in Chesapeake Bay (US Army ERDC 2000). ICM stands for "integrated compartment model," which is analogous to the finite volume numerical method. The model computes and reports concentrations, mass transport, kinetics transformations, and mass balances. This eutrophication model computes 22 state variables including multiple forms of algae, carbon, nitrogen, phosphorus, and silica, and dissolved oxygen. One significant feature of ICM is a diagenetic sediment sub-model, which interactively predicts sediment-water oxygen and nutrient fluxes. Alternatively, these fluxes may be specified based on observations.

The foundation of CE-QUAL-ICM is the solution to the three-dimensional mass-conservation equation for a control volume based on the finite volume approach. Transport within the CE-QUAL-ICM (Cerco and Cole 1995) is based on the integrated compartment method (or box model methodology). The present version of CE-QUAL-ICM transport is a loose extension of the original WASP code (Ambrose et al. 1986). The notion of utilizing the box model concept was retained in order to allow the coupling, via map files, of ICM with various hydrodynamic models. ICM represents "integrated compartment model," which is the finite volume numerical method. The model computes constituent concentrations resulting from transport and transformations in well-mixed cells that can be arranged in arbitrary triangular and quadrilateral configurations.

Water quality data including dissolved oxygen, chlorophyll-a, TKN, ammonium, nitrate-nitrite, and total phosphorus were collected by the Virginia Department of Environmental Quality (VA-DEQ) at its 16 Lynnhaven stations over the 3-year period 2004-2006. The successful calibration and validation of the CE-QUAL-ICM model for the Lynnhaven River is confirmed by the quality of comparisons of model predictions to these data, as reported by Sisson et al. (2010b), available online at: http://www.vims.edu/greylit/vims/sramsoe408.pdf

The goal of this study was to obtain critical data necessary for incorporating the effects of oyster reefs on nutrient and sediment dynamics into the CE-QUAL-ICM water quality model for the Lynnhaven River. Our specific objectives were to estimate (1) oyster filtration rates, (2) biodeposition rates, (3) nutrient flux rates between the sediment and water column, and (4) nutrient sequestration in relation to oyster biomass on reefs in the Lynnhaven River, with the intent that these would then be used in subsequent work to incorporate these effects into the water quality model to predict system-wide effects of oysters on water quality.

CHAPTER II. METHODS

II-1 Study Sites

Experiments to determine the relationship between oyster biomass (and abundance) and both nutrient fluxes and standing stock sequestration were conducted at four sites in the Lynnhaven River (Fig. II.1). The Humes Marsh site (Fig. II.1 A) is an intertidal muddy sand flat that is leased by Mr. John Meekins for the purpose of oyster cultivation.   Mounds of planted oyster shell serve as settlement substrate for wild oysters at this site (Fig. II.2).
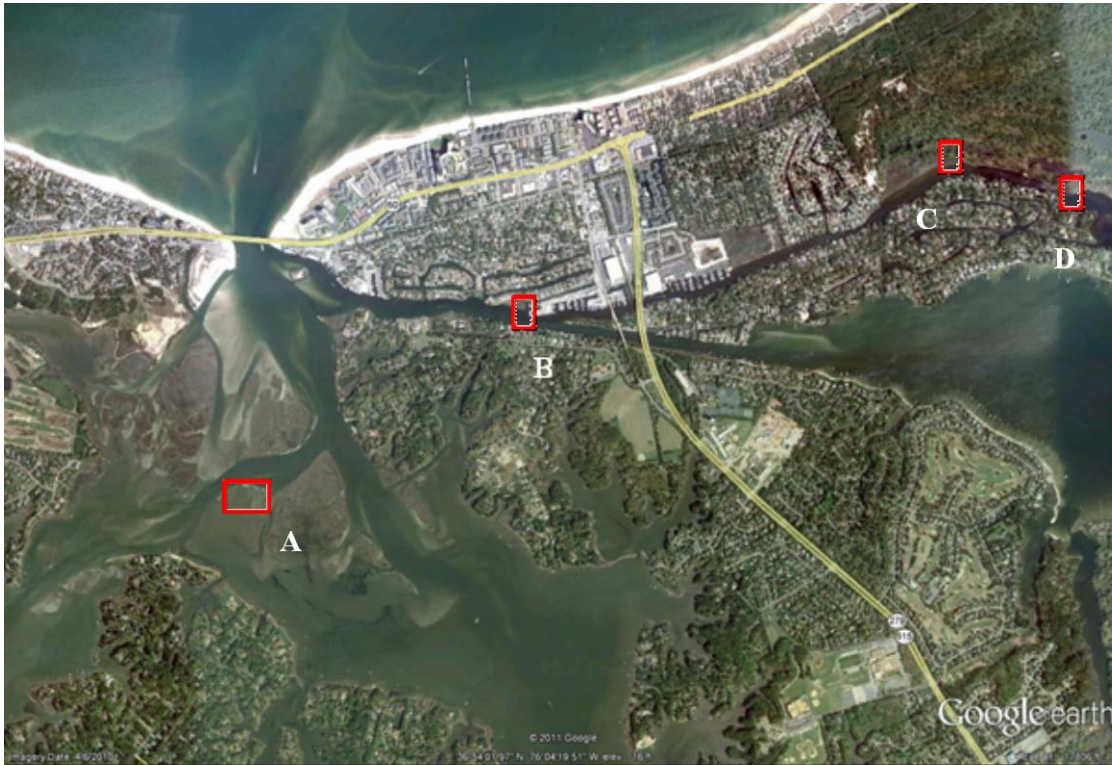
Figure II.1. Study sites in the Lynnhaven River used for deploying nutrient flux chambers on oyster reefs with varying oyster density. (A) Humes Marsh site, (B) One Fish, Two Fish site, (C) West Long Creek site and (D) East Long Creek site.

These shelled areas support oysters reefs with varying densities of oysters ranging from 10's to 100's per m^2. Areas between the mounds of shell include bare sediment habitat and isolated clumps of oysters on bare sediment.

Three sites, located in Long Creek (Fig. II.1 B-D), contained oyster reefs with different configurations. The westernmost study site in Long Creek (Fig. II.1 B) is an intertidal sandy mudflat located near the One Fish, Two Fish Restaurant. This site (hereafter referred to as One Fish, Two Fish) contains scattered clumps of oysters on an otherwise soft-sediment bottom (Fig. II.3) that is typical of many areas within the intertidal zone of the Lynnhaven River. The other two sites in Long Creek (Fig. II.1 C & D) are located in the shallow

subtidal zone on shells planted by the Virginia Marine Resources Commission (VMRC) as part of an oyster restoration program. One of these sites (Fig. II.1 C) has sparse clumps of oysters on a primarily mud bottom, while the other site (Fig. II.1 D) has a more uniform base of oyster shell and relatively low densities of oysters.

Figure II.2. Intertidal oyster reefs at Humes Marsh. Note the reef in the foreground and several reefs in the background separated by bare sediment habitat.

Figure II.3. Intertidal oyster clumps on a sandy-mud bottom near One Fish, Two Fish Restaurant.

Using these four sites we identified a total of eight sample locations based upon nominal oyster density (none, low, medium or high), tidal exposure (intertidal or subtidal) and base substrate type (shell or soft-sediment) for determination of nitrogen fluxes and nutrient sequestration (Table II.1). Our intention in picking these sample sites was to allow us to obtain measurements of nitrogen fluxes and nitrogen and phosphorus sequestration in relation to oyster density and biomass, while at the same time teasing out the effects of intertidal vs. subtidal and shell vs. barren bottom. Determining the full effects of each of these factors would have required many more densities and station replicates than were possible in the context of this study. Budgetary and time constraints limited us to running nine incubation chambers (described below) as part of this study. The eight stations described in Table II.1 plus one required water blank represent the most efficient use of resources for meeting the study objectives.

Table II.1. Description of sample stations.

Location	Station Code	Tidal Elevation	Base substrate	Density category
Humes Marsh				
	HM0	Intertidal	Sediment	None
	HMLsed	Intertidal	Sediment	Low
	HML	Intertidal	Shell	Low
	HMM	Intertidal	Shell	Medium
	HMH	Intertidal	Shell	High
One Fish Two Fish				
	1F2F	Intertidal	Sediment	Low
Long Creek West				
	LCW	Subtidal	Sediment	Low
Long Creek East				
	LCE	Subtidal	Shell	Low

II-2 Measurement of Oyster Reef Biogeochemical Fluxes

The sediment-water exchange of substances generally requires sealing a portion of the sediment community into a chamber, either *in situ* (e.g. benthic landers) or *ex situ* (i.e. cores), and measuring the change of solute or gas concentration over time (Cowan & Boynton 1996; Cornwell et al. 1999; Hammond et al. 2004). Alternative approaches include measuring differences in inflow and outflow concentrations in flow-through incubations (Miller-Way et al. 1994; Piehler and Smyth 2011) and *in situ* measurements of oxygen fluxes using eddy correlation (Berg et al. 2003). Our incubation chambers, described below, are designed to provide realistic field conditions from *in situ* equilibrations with high-precision measurements from *ex situ* incubations and measurements.

II-3 Incubation Chamber Design

Our experimental flux chambers (hereafter "chambers") are described in detail in Kellogg et al. (2011). Briefly, each consists of three sections machined from 40.6-cm (16") outer diameter PVC pipe and two types of lids (Table II.2, Fig. II.4). *Base trays* were constructed from a disk of PVC glued to a 10.1-cm section of PVC pipe resulting in an inner height of 8.9 cm (Fig. II.4.A.1). Each base tray was paired with a *midsection* consisting of an 18.5-cm section of PVC pipe (Fig. II.4.A.2). To turn this section into a watertight cap (hereafter "transport lid") for use during retrieval of base trays from the field, a PVC disk edged with an O-ring was inserted into the top of this section of pipe. During incubations, the midsection of each chamber was topped with an *upper section* consisting of a 13.8-cm section of PVC, bringing the total height of the chamber to 42.6 cm (Fig. II.4.A.3). Each chamber was sealed with a removable stirring lid (Fig. II.4.A.4 and II.4.B) constructed of transparent PVC with two ports that allowed samples to be drawn and water to be replaced during experiments. An additional port allowed insertion of a dissolved oxygen probe (NexSens Model #: WQ-DO) for tracking of dissolved oxygen concentration throughout the course of experiments. A 12V motor connected to a drive disk with embedded magnets mounted on the exterior of the

stirring lid. A matching drive disk connected to a drive shaft with two impellers was mounted on the interior of the stirring lid. Using this apparatus precluded the need for a drive shaft to pass through the lid and allowed us to turn the impeller while preventing exchange of gases between the chamber and the water bath. During incubations, the impellers turned at 71-76 RPM, which was sufficient to achieve vertical mixing of the water column without resuspending bottom sediments in the chamber.

Table II.2. Chamber dimensions. Diameter is reported as average ± SD because variation in materials resulted in minor differences in tray diameter (N = 9).

Component	Dimensions (cm)	
Base tray diameter	37.7	± 0.2
Base tray inside height	8.9	
Total chamber height (3 sections)	42.6	
Length of impeller bars, tip to tip	24.0	
PVC pipe thickness	1.3	

II-4 Nutrient Flux Measurements

Nutrient fluxes were measured for the sites described in Table II.1 during the fall of 2011. Chamber bases were deployed at the field sites as described below on September 13 and 14. Chamber bases were then retrieved on October 17 and transported to the VIMS Eastern Shore Laboratory where the chambers were incubated and water samples collected over a 6.5-hr period. Dissolved gases and solutes in these water samples were then measured to determine fluxes. The methods for determining fluxes are summarized in Table II.3 and described in greater detail below.

Field deployment and retrieval - One chamber base tray was deployed around low tide at each of the sample locations. Prior to deployment, oyster populations at each location were sampled to determine abundance, size, and biomass density of oysters at each site. Haphazardly-located replicate quadrat samples were collected at each site, by removing all of the oysters within a quadrat. Both quadrat size (0.0625 m^2 to 1.00 m^2) and the number of replicate quadrats (3 to 8) varied depending upon the density and underlying distribution of oysters at a site. Oysters were transported to the laboratory where they were enumerated, shell height measured to the nearest mm, and dry weight biomass of soft tissues and shell determined.

After the surveys were completed, a chamber base tray was embedded in the substratum with ~2.5cm of the tray extending above the sediment-water interface. To embed each tray, material from the reef (or bare sediment in the case of the control) was placed in the tray and the tray placed in the resulting depression (Fig. II.5). Once deployment was complete, trays remained in the field for 33 - 34 days to allow the system (oysters, associated fauna, biodeposits, and microbial community) to equilibrate with the surrounding reef. For three days prior to the retrieval date, a YSI 6600 meter was deployed near the Humes Marsh site to record temperature, salinity and dissolved oxygen concentrations.

At the end of the equilibration period, base trays were retrieved from all sites and returned to the Virginia Institute of Marine Science's Eastern Shore Laboratory (ESL) in Wachapreague, VA. Before retrieval, trays were capped underwater using the chamber midsection and the

9

transport lid (Fig. II.4.A, sections 2 & 3) that allowed collection of the reef materials, associated organisms, sediments, and a portion of the overlying water column. After capping, the trays were removed, returned by boat to the dock, and transported in 200-L water baths by truck to Wachapreague.

Figure II.4. Photographs of an incubation chamber. A) Complete chamber as it was configured for incubations. Chamber components (labeled in red) are: (1) base tray, (2) midsection, (3) upper section, and (4) stirring lid. B) Photograph of the stirring bar and shaft that extend into experimental chamber.
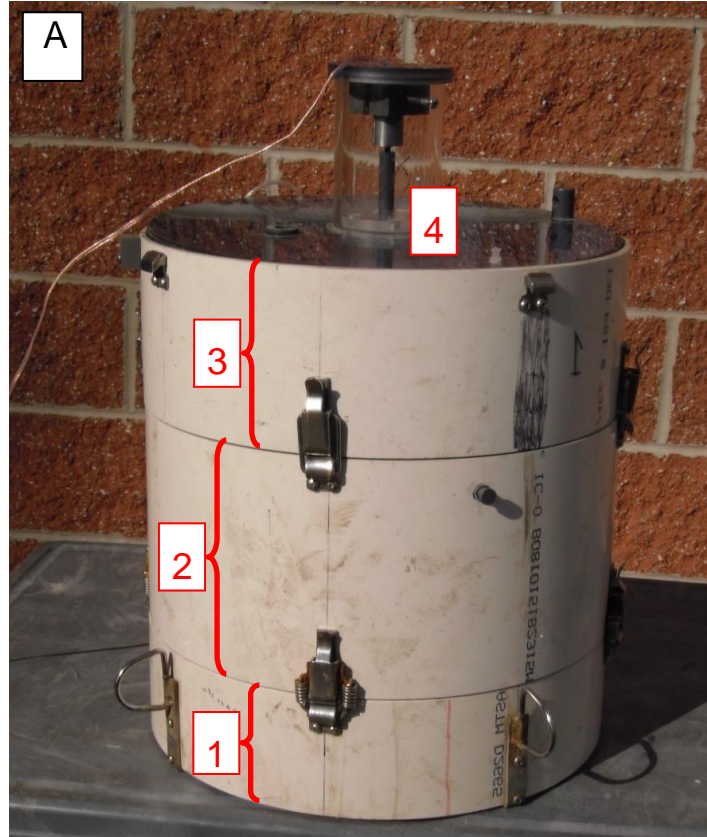
Table II.3. Synopsis of flux measurement approach

Sampling Design	Seven oyster reefs spanning a range of densities and bottom types and one bare sediment habitat within the Lynnhaven River were selected for measuring nutrient fluxes and estimating nutrient sequestration in relation to oyster density. Quantitative samples were taken to determine oyster density and biomass at each site.
Tray Deployment	Incubation chamber base trays were deployed at haphazardly-selected locations within each study site. Each of the 8 trays was filled with material from the site and embedded flush with surrounding sediments.
Tray Collection	After ~ 1 month, the trays were capped using the midsection of the incubation chamber fitted with the transport lid. Capped trays were then transported to the VIMS Eastern Shore Lab (ESL) for processing.
Water for Incubation	Unfiltered seawater from Wachapreague Channel was mixed with freshwater and temperature controlled to match conditions in the Lynnhaven (20 psu and 20 °C).
Incubation Facility	Samples were incubated in a temperature controlled water bath at the ESL. Light was controlled for light and dark incubations.
Pre-Incubation	In the lab, the transport lid was removed from the midsection of each chamber and the upper section of the chamber was locked into place. Chambers were placed in a water bath, carefully filled with prepared seawater water, and bubbled with air for ~1 hour to ensure dissolved oxygen levels reached saturation and to establish thermal equilibrium. A complete water change was made prior to the start of incubation to ensure that NH_4 and other metabolites were at background levels prior to initiation. During aeration and water changes, a 500-μm mesh lid was placed on each chamber to prevent escape of mobile macrofauna. Pre-incubations were carried out in the dark.
Incubation	For incubations, mesh lids and air stones were removed and chambers were capped with O-ring sealed stirring lids. Care was taken to exclude bubbles. NexSens recording oxygen/temperature electrodes were placed in all chambers. PVC tubing was attached to two ports on the stirring lid; one line was attached to a peristaltic pump for sample collection and the other drew replacement water from the water bath into the chamber. The first incubation was carried out in the dark, followed by a water change and then a second incubation in the light.
Sample Collection and Preservation	At intervals based upon real-time oxygen data, samples were collected for gas and solute analyses. Prior to each sampling event, pumps were used to purge the sampling lines. During each sampling event, water samples were collected for analysis of dissolved gases (oxygen, di-nitrogen and argon) and solutes (soluble reactive phosphorus, ammonium, and combined nitrate and nitrite). Dissolved gas samples were collected in 7-ml glass test tubes, preserved with $HgCl_2$, sealed with ground glass stoppers, submerged in water, and stored at ≤ incubation temperature. Solute samples were collected and placed in 60 ml syringes, filtered to remove particulates, and immediately frozen in replicate 7-ml vials until analysis.
Sample Analysis	Dissolved gas samples were analyzed using membrane inlet mass spectrometry and were processed within one week of collection. Solute samples were analyzed using wet chemical and auto-analyzer techniques.

Figure II.5. Examples of chamber base trays embedded in the bottom at sample sites in the Lynnhaven. (A) Low oyster density with shell bottom site at Humes Marsh, (B) High oyster density with shell bottom site at Humes Marsh, (C) Low oyster density with sandy mud bottom at One Fish, Two Fish site, (D) Bare sediment site at Humes Marsh.
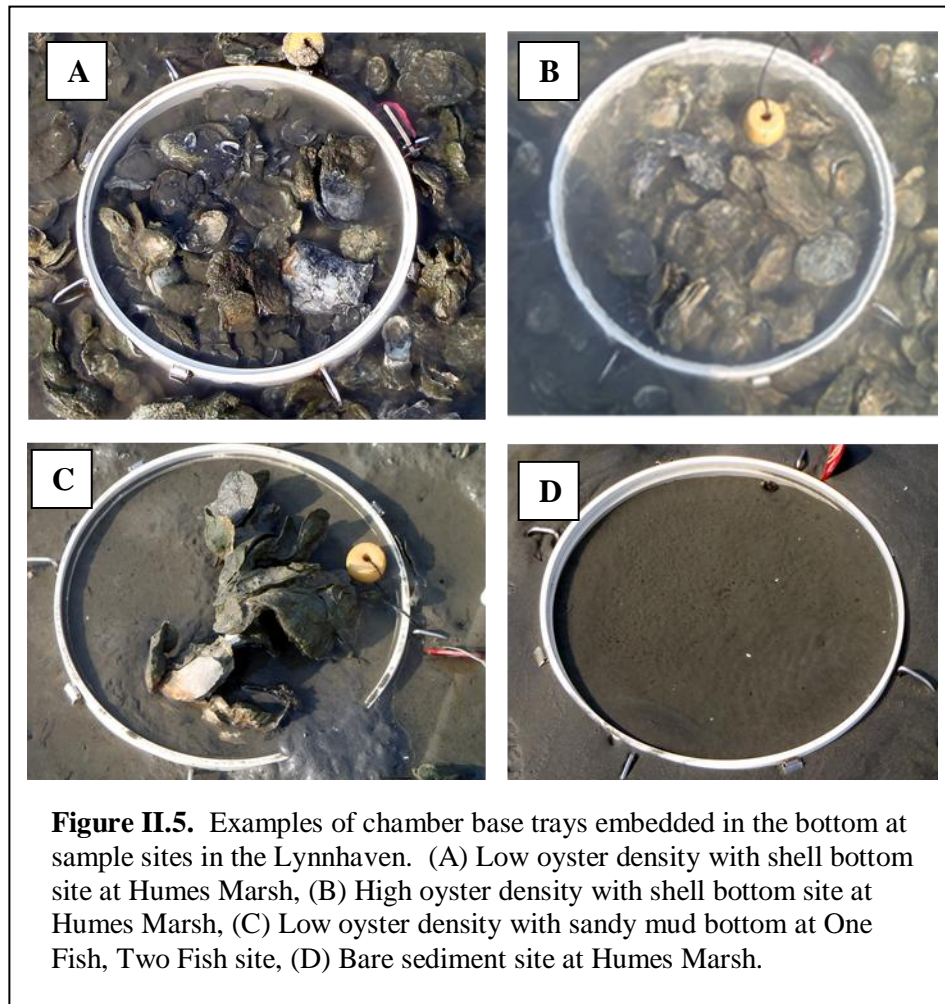
Sample incubations – All chambers were delivered to the VIMS-ESL within three hours of collection from the field. More than 24 hours prior to the expected arrival of the chambers, holding tanks in the laboratory were filled with a mixture of unfiltered seawater from Wachapreague Channel and freshwater to match the salinity at the Lynnhaven River sites. Seawater temperature in the holding tanks was maintained at the measured temperature at the time of retrieval in the Lynnhaven. Upon arrival at the ESL, the transport lid was removed from the midsection of each chamber and the upper section of the chamber was locked into place (Fig. II.4.A.3). Chambers were then placed in the water bath, carefully filled with prepared water, and bubbled with air for >1 hour to bring dissolved oxygen levels to saturation. During aeration, a 500-µm mesh lid was placed on each chamber to prevent escape of mobile macrofauna. An empty chamber was also placed in the water bath and served as a seawater control (hereafter "blank"), bringing the total number of chambers sampled during each set of experiments to nine. Prior to the start of the incubations, water in the baths was drained and replaced with water from the holding tanks to ensure that levels of ammonia and other compounds were similar to background levels at the start of incubations.

Incubations were conducted under both light and dark conditions. Dark incubations began within 5 hours of collection of the first sample in the field and were followed by incubations under light conditions. Prior to starting the incubations, mesh lids and air stones were removed from chambers and replaced with stirring lids. Because respiration rates were expected to be highest in chambers containing the highest oyster biomass, the seawater blank chamber and the chambers with lower oyster biomass were sealed with stirring lids before the chambers with higher oyster biomass. Each stirring lid was edged with an O-ring and fitted with a sampling line, a water replacement line, and a dissolved oxygen probe. The sampling line consisted of 3.2-mm inner diameter PVC tubing; one end was attached to a port on the chamber lid and the other to a peristaltic pump. The water replacement line was constructed of the same tubing and drew replacement water from the water bath in which the chamber was immersed. An oxygen electrode (NexSens Model #: WQ-DO) was inserted into each chamber lid through an O-ring sealed port (Fig. II.6). During sealing of chambers with stirring lids, care was taken to ensure that no gas bubbles were trapped in the chamber.

During incubations, we sampled solutes and dissolved gases a minimum of five times in each chamber. Timing of sampling events was adjusted based upon data collected every 30 seconds by dissolved oxygen probes and displayed on laptop computers. Between the dark and light incubation periods, stirring lids were replaced with mesh lids with air stones and aerated for >1 h to return oxygen levels to saturation. Just prior to the start of the light incubation, water was drained from the water baths and replaced.

During each sampling event of both incubations, water samples were collected for dissolved gas (oxygen, di-nitrogen, and argon) and dissolved nutrient (soluble reactive phosphorus, ammonium, and combined nitrate

Figure II.6. Incubation chambers with stirring lids in place in the water bath. Dissolved oxygen probe and sample lines are visible penetrating the chamber lid.

and nitrite) analyses. Prior to each sampling event, pumps were used to purge the sampling lines for several minutes to ensure that water remaining in the lines from previous sampling was not included in the sample. Water samples were then collected simultaneously from chambers using two Rainin 8-channel peristaltic pumps. Dissolved gas samples were collected in 7-ml glass test tubes, preserved with using 10μL of 50% saturated $HgCl_2$ to prevent biological transformations, sealed with ground-glass stoppers, submerged in water, and stored at temperatures equal to or below incubation temperatures. Nutrient samples were collected and placed in 60-ml syringes, filtered using syringe filters (pore size = 0.45 μm), and frozen in individual 7-ml polycarbonate vials until analysis.

Water sample analyses - Water samples collected during incubations were analyzed to determine net fluxes of oxygen (O_2), di-nitrogen (N_2), soluble reactive phosphorus (SRP), ammonium (NH_4^+), and combined nitrate and nitrite (NO_{2+3}). Although different techniques were used to analyze the samples, fluxes for all analytes were determined using linear

regressions fitted to plots of concentration versus time. To remove the influence of water column processes from our results, slopes of regression lines were adjusted using data from the blank chamber when these data indicated a significant flux of an analyte. Fluxes were considered significant when the regression line had an R-squared value ≥0.80 and the difference between data in a time course was greater than the precision of the method used for analysis.

Membrane inlet mass spectrometry - Membrane inlet mass spectrometry, a high-precision rapid method for analyzing concentrations of dissolved gases (Kana et al. 1994), was used to determine the concentrations of N_2 and O_2 in our samples. Briefly, each sample was analyzed by bringing it to constant temperature, pumping it at a constant rate through a silicone membrane in the vacuum inlet of a quadrupole mass spectrometer, monitoring the signals from the mass spectrometer for N_2, O_2, and argon (Ar), constantly calculating gas ratios (N_2:Ar and O_2:Ar) until they stabilized, and recording these stable values. In practice, this technique yields coefficients of variation for gas ratios of ~0.02%. During the first sampling event of the dark incubation, duplicate samples were collected and replicate analyses were conducted and used as an internal precision check of the method.

Solute analysis - All dissolved nutrient analyses were carried out by the Analytical Services laboratory at Horn Point Laboratory following standard procedures. Soluble reactive phosphorus (SRP) was analyzed using a phosphomolybdate colorimetric analysis (Parsons et al. 1984) with a detection limit of <0.005 mg L^{-1}. NH_4^+ concentrations were determined using phenol/hypochlorite colorimetry (Parsons et al. 1984). Combined NO_{2+3} concentrations were determined using Cd reduction of NO_3 to NO_2 with a detection limit of <0.03 mg L^{-1} (Parsons et al. 1984).

II-5 Nutrient sequestration

Once incubations were complete, stirring lids were removed and samples were again aerated and capped with 500‑μm mesh lids. Chambers were then held in the water bath until they were processed to collect all macrofauna retained on a 1.0-mm sieve. While chambers awaited processing, bath water was replaced as needed with salinity-adjusted, filtered seawater from Wachapreague Channel.

<u>*Macrofaunal Abundance and Biomass*</u> - Macrofauna were collected by rinsing all of the substrate in the incubation chambers through a 1.0-mm mesh sieve. Oyster shells were carefully broken apart and rinsed in freshwater to remove polychaetes (primarily *Allita succinea*) that are often found within interstitial space within the shell. Larger macrofauna and macrofauna attached to large oysters shells were frozen for later analyses. All other material retained on the sieves was fixed in 10% buffered formalin. After a minimum of 48 hours in formalin, samples were rinsed thoroughly and transferred to 70% ethanol. All organisms in both frozen and preserved samples were then identified to the lowest practical taxonomic level and enumerated. Dry weight biomass for whole organisms was then determined by drying at 60 °C for a minimum of 48 hours and weighing to the nearest 0.1 mg. For oysters, ribbed mussels (*Geukenisia demissa*) and hard clams (*Mercenaria mercenaria*), soft tissue was first removed from the shell and dry weights were determined separately for shell and soft tissue for all but the smallest individuals.

Macrofaunal Nutrient Content - Nitrogen and phosphorus content for each major faunal group in our samples were estimated by one of two methods. For those faunal groups analyzed by Kellogg et al. (2011) previously determined values for N and P as percentages of dry weight biomass were used. For other faunal groups, we haphazardly selected a minimum of three individuals from each group and the VIMS Analytical Services Laboratory analyzed nitrogen content using a CHN analyzer and phosphorus content using colorimetric analysis. Nitrogen and phosphorus content were then reported as a percent of dry tissue weight and total N and P sequestered by macrofauna in the sample determined by multiplication.

II-6 Biomass-specific oyster filtration and biodeposition rates

Biodeposition and biofiltration rates were analyzed from a database generated by Jordan (1987). This is a unique data set that was never published in the peer-reviewed scientific literature, and which was derived from a series of mesocosm studies that examined biodeposition rates of the eastern oyster as a function of seston concentration, water temperature, and salinity (Jordan 1987). We re-analyzed the data using non-linear regression models. In addition, we evaluated the available literature on biodeposition and biofiltration rates most relevant to the project goals.

II-7 Statistical analyses

Following square root transformation to meet the assumption of normality, we tested for differences between abundance and biomass density of oysters at each of the study sites using one-way ANOVAs. Pairwise multiple comparisons tests with an experiment-wise error rate=0.05 were then used to identify significant differences in abundance and in biomass between our eight sampling stations.

CHAPTER III. RESULTS

III-1 Oyster density and biomass

The abundance and dry weight biomass density of oysters at each of our stations is reported in Table III.1. One-way ANOVAs on square root-transformed data revealed significant differences among stations in oyster density (F=42.581, d.f.=6, p<0.001) and biomass (F=31.725, d.f.=6, p<0.001). The sites that we categorized as low oyster density on soft-sediment bottom types at Humes Marsh, One Fish Two Fish and West Long Creek had comparable oyster densities and biomass. The low oyster density sites on shell bases at Humes Marsh and East Long Creek had moderately higher densities of oysters, but these were not significantly different from the other low density sites on sediment.   Both oyster abundance and biomass on the medium and high density oyster reefs at the Humes Marsh site were not significantly different from one another, but were $5 - 10$ times greater than those at the low density sites (Table III.1).

Table III.1. Measured oyster density and biomass at each sample site. Values in parentheses are one standard deviation. Lower case letters in the last column indicate significant differences between stations for both oyster density and biomass as determined by the pairwise multiple comparisons tests (Holm-Sidak method, experiment-wise error rate ≤ 0.05).

Location	Station Code	Tidal Elevation	Base substrate	Density category	Measured oyster density	Measured oyster biomass	Sig. density/ biomass
Humes Marsh					# m^{-2} (SD)	g m^{-2*}(SD)	
	HM0	Intertidal	Sediment	None	0	0	a
	HMLsed	Intertidal	Sediment	Low	46.7 (26.6)	35.4 (30.4)	b
	HML	Intertidal	Shell	Low	124 (64.5)	117.3 (69.1)	b
	HMM	Intertidal	Shell	Medium	480 (91.8)	322.9 (103.2)	c
	HMH	Intertidal	Shell	High	576 (1632)	370.8 (77.6)	c
One Fish Two Fish							
	1F2F	Intertidal	Sediment	Low	54.5 (9.6)	42.9 (9.4)	b
Long Creek West							
	LCW	Subtidal	Sediment	Low	61.3 (10.1)	49.1 (7.9)	b
Long Creek East							
	LCE	Subtidal	Shell	Low	115 (55.6)	43.7 (16.9)	b

Modal shell height of oysters at all sites ranged between 40 and 60 mm and all sites had some oysters over 100 mm (Fig. III.1). Substantial portions of the oysters at all sites exceeded the legal harvest size of 76 mm. This is particularly relevant at the Humes Marsh site that is commercially harvested by a private leaseholder.
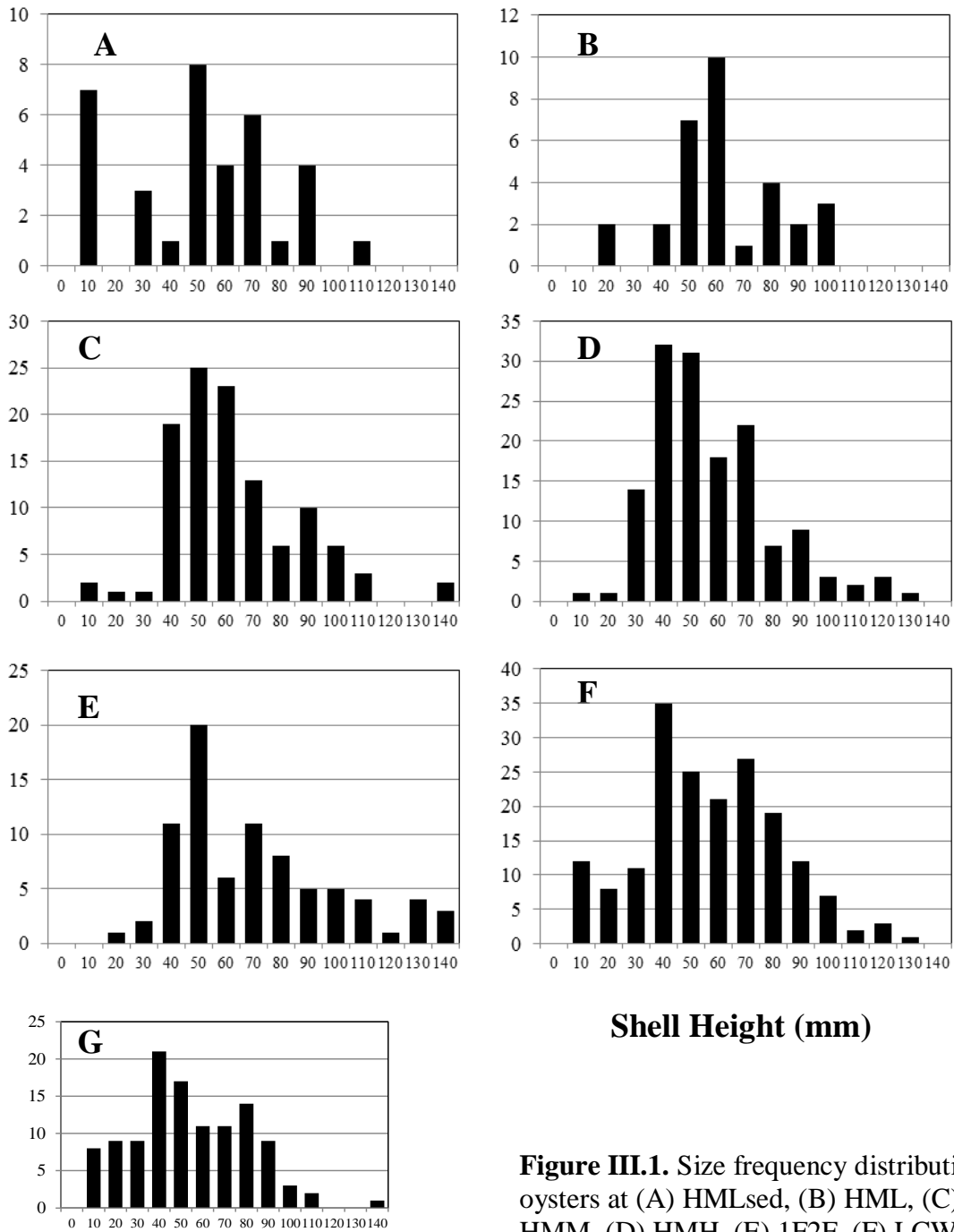
Shell Height (mm)

Figure III.1. Size frequency distribution of oysters at (A) HMLsed, (B) HML, (C) HMM, (D) HMH, (E) 1F2F, (F) LCW and (G) LCE. Station codes are as in Tables II.1 & III.1.

Shell Height (mm)

III-2 Macrofauna biomass

The foregoing section reported oyster density, biomass, and shell height from quadrat samples taken at each field site at the time of base tray deployment. In addition, following the chamber incubations, we determined the abundance and biomass of all infaunal and epifaunal macrobenthic and demersal organisms in the chamber base trays returned to the laboratory (Tables III.2 and III.3). These data reveal similar patterns among the study sites in oyster abundance and biomass to those observed in the quadrat samples. The high and medium density sites at Humes Marsh generally had greater oyster biomass than the other sites, with the exception of the chamber from the 1F2F site that contained many small oysters. The HMH incubation chamber contained more than twice as many oysters as the HMM chamber (Table III.2); however, the oysters in the latter were larger and oyster biomass in the two treatments was similar (Table III.3).

Table III.2. Macrofauna abundance (g m^{-2}) by taxa from each site. Data are derived from the fauna in the incubation chambers.

	Station							
	HM0	HMLsed	HML	HMM	HMH	1F2F	LCW	LCE
Bivalves								
Crassostrea virginica	0	172	213	502	1,150	546	250	136
Geukensia demissa	0	0	53	63	178	0	0	0
Mercenaria mercenaria	0	9	35	18	27	9	0	0
Small clams (<10 mm)	18	81	44	99	116	0	0	0
Anomia simplex	0	9	9	0	0	0	9	0
Gastropods								
Crepidula spp.	0	181	89	54	0	0	71	72
Ilyanassa obsoleta	205	18	0	0	0	0	0	0
Crustaceans								
Amphipods	9	0	27	0	348	9	0	715
Barnacles	0	4,228	3,749	19,852	10,640	446	62	208
Blue Crab	0	9	9	0	0	9	0	0
Hermit crab	0	0	0	9	0	0	0	0
Xanthid Crabs	0	235	363	466	855	127	62	235
Grass Shrimp	0	27	27	18	0	0	0	290
Snapping Shrimp	0	0	0	0	0	0	18	127
Other								
Polychaetes (mostly *Alitta succinea*)	45	91	186	90	285	55	98	118
Molgula manhattensis	0	905	239	412	223	0	0	154
Gobiosoma bosci	0	9	9	45	0	9	27	100

Barnacles were the most numerous non-oyster macrofauna found at the sites with oysters, followed by polychaetes and tunicates (Table III.2). The biomass dominant organisms (exclusive of oysters) from these sites were hard clams, *M. Mercenaria,* followed by barnacles and ribbed mussels (*G. demissa*). At the control site without oysters, mud snails (*Ilyanassa obsoleta*) were both the numeric and biomass dominant species.

Table III.3. Macrofauna biomass density (g m^{-2}) by taxa from each site. Data are derived from the fauna in the incubation chambers.

Taxon	Station							
Bivalves	HM0	HMLsed	HML	HMM	HMH	1F2F	LCW	LCE
Crassostrea virginica								
Shell	0.00	1,564.83	5,713.94	12,076.91	9,810.66	5,172.48	2,328.71	410.15
Tissue	0.00	61.04	130.30	356.63	196.84	184.87	577.35	10.13
Geukensia demissa								
Shell	0.00	0.00	31.33	141.89	187.36	0.00	0.00	0.00
Tissue	0.00	0.00	3.16	11.38	11.72	0.00	0.00	0.00
Whole Organism	0.00	0.00	0.18	0.19	0.00	0.00	0.00	0.00
Mercenaria mercenaria								
Shell	0.00	348.46	1,779.45	1,139.64	2,715.42	0.00	0.00	0.00
Tissue	0.00	14.74	748.90	31.06	97.22	0.00	0.00	0.00
Whole Organism	0.00	0.00	0.00	0.00	0.00	0.06	0.00	0.00
Small clams (<10 mm)	0.11	1.91	0.47	0.23	0.29	0.00	0.00	0.00
Anomia simplex	0.00	1.51	27.55	0.00	0.00	0.00	0.45	0.00
Gastropods								
Crepidula spp.	0.00	5.73	5.26	0.18	0.00	0.00	3.43	1.42
Ilyanassa obsoleta	378.53	30.02	0.00	0.00	0.00	0.00	0.00	0.00
Crustaceans								
Amphipods	0.00	0.00	0.01	0.00	0.55	0.01	0.00	0.18
Barnacles	0.00	37.80	34.67	324.78	145.83	6.82	0.42	6.63
Blue Crab	0.00	0.43	0.64	0.00	0.00	0.28	0.00	0.00
Hermit crab	0.00	0.00	0.00	16.38	0.00	0.00	0.00	0.00
Xanthid Crabs	0.00	5.33	21.70	68.68	76.71	59.04	3.15	81.38
Grass Shrimp	0.00	0.42	0.22	0.43	0.00	0.00	0.00	6.78
Snapping Shrimp	0.00	0.00	0.00	0.00	0.00	0.00	4.48	8.00
Other								
Polychaetes (mostly *Alitta succinea*)	1.41	2.07	0.69	0.83	2.15	0.40	1.57	0.66
Molgula manhattensis	0.00	14.22	1.21	3.38	1.27	0.00	0.00	0.52
Gobiosoma bosci	0.00	0.31	0.40	4.15	0.00	1.32	1.45	5.23
Total biomass	**380.04**	**2088.81**	**8500.10**	**14176.73**	**13246.02**	**5425.29**	**2921.01**	**531.06**

III-3 Nutrient sequestration in macrofauna

Nitrogen content of the soft tissues in bivalves ranged from 5.96% to 9.27% of dry weight, while shells contained a much lower percentage of nitrogen (0.15 % to 0.64%) by weight (Table III.4). Similarly, shells contained a much lower percentage of phosphorus (0.002 to 0.040%) than did soft tissues (1.260% to 0.511%). Whole organism nitrogen content among the other macrofauna found in our samples ranged one order of magnitude from approximately 1% to 10% of dry weight biomass and phosphorus content varied roughly two orders of magnitude from 0.037% to 3.61% of dry weight (Table III.4).

Table III.4. Nitrogen and phosphorus conversions as a percent of dry weight.

Taxon	Source	%N	%P
Bivalves			
Crassostrea virginica			
Shell	Kellogg et al. 2011	0.21	0.040
Tissue	Kellogg et al. 2011	9.27	1.260
Geukensia demissa			
Shell	Present Study	0.64	0.016
Tissue	Present Study	8.81	0.670
Mercenaria mercenaria			
Shell	Present Study	0.15	0.002
Tissue	Present Study	5.96	0.511
Small clams (<10 mm)	Kellogg et al. 2011	1.42	0.100
Anomia simplex[a]	Kellogg et al. 2011	1.42	0.100
Gastropods			
Crepidula spp.[b]	Present Study	0.94	0.037
Ilyanassa obsoleta	Present Study	0.94	0.037
Crustaceans			
Amphipods	Kellogg et al. 2011	4.53	1.990
Barnacles	Kellogg et al. 2011	0.99	0.140
Blue Crab	Present Study	5.15	1.199
Hermit crab	Present Study	5.87	0.942
Xanthid Crabs	Kellogg et al. 2011	3.98	1.370
Grass Shrimp	Kellogg et al. 2011	9.35	2.590
Snapping Shrimp	Present Study	7.86	1.213
Other			
Polychaetes (mostly *Alitta succinea*)	Kellogg et al. 2011	6.84	1.070
Molgula manhattensis	Present Study	3.40	0.306
Gobiosoma bosci	Kellogg et al. 2011	10.60	3.610

[a] Values estimated using data for small clams

[b] Values estimated using data for mud snails

Multiplying the percent nitrogen and phosphorus content for each taxonomic group by its density from each site yields estimates of the amount of nitrogen (Table III.5) and phosphorus (Table III.6) sequestered in macrofaunal organisms at the time of our sampling.

Table III.5. Nitrogen sequestration (g m^{-2}) by taxa from each site. Data are derived from the fauna in the incubation chambers.

Taxon	Site							
Bivalves	HM0	HMLsed	HML	HMM	HMH	1F2F	LCW	LCE
Crassostrea virginica								
Shell	0	3.286	11.9993	25.361	20.602	10.862	4.89	0.861
Tissue	0	5.658	12.0789	33.060	18.247	17.138	53.520	0.939
Geukensia demissa								
Shell	0	0	0.2005	0.908	1.1991	0	0	0
Tissue	0	0	0.2785	1.003	1.0323	0	0	0
Whole organism			0.014	0.015	<0.001			
Mercenaria mercenaria							0	0
Shell	0	0.523	2.669	1.710	4.0731	0	0	0
Tissue	0	0.8785	44.635	1.851	5.7945	0	0	0
Small clams (<10 mm)	0.0015	0.027	0.007	0.003	0.0041	0	0	0
Anomia simplex	0	0.021	0.3913	0	0	0	0.06	0
Gastropods								
Crepidula spp.	0	0.0538	0.049	0.002	0	0.00	0.032	0.013
Ilyanassa obsoleta	3.5581	0.2822		0	0	0.00	0	0
Crustaceans								
Amphipods	0.0001	0	0.001	0	0.0249	0.001	0	0.008
Barnacles	0	0.374	0.343	3.215	1.4437	0.068	0.004	0.066
Blue Crab	0	0.0220	0.033	0	0	0.014	0	0
Hermit crab	0	0	0	0.961	0	0.00	0.00	0
Xanthid Crabs	0	0.212	0.864	2.733	3.0529	2.350	0.126	3.239
Grass Shrimp	0	0.040	0.021	0.040	0	0	0	0.634
Snapping Shrimp	0	0	0	0	0	0	0.352	0.629
Other								
Polychaetes (mostly *Alitta succinea*)	0.0962	0.142	0.69	0.564	0.147	0.027	0.107	0.045
Molgula manhattensis	0	0.491	1.21	0.117	0.044	0.00	0	0.018
Gobiosoma bosci	0	0.033	0.40	0.439	0	0.140	0.154	0.554
Total	**3.656**	**12.044**	**73.702**	**71.460**	**55.665**	**30.600**	**59.192**	**7.006**

Total nitrogen sequestration in macrofauna, as estimated from our samples, was greatest at the HML site, largely as a consequence of the inclusion of several large clams, *M. mercenaria*, in the sample. The inclusion of a few large oysters in the LCW incubation

chamber resulted in soft tissue biomass (Table III.3), nitrogen (Table III.5) and phosphorus (Table III.6) content that was likely higher than the average for that site. Despite a lower percent content of nitrogen in shells relative to soft tissue in bivalves, the greater total mass of shell resulted in comparable amounts of nitrogen being stored in shells and soft tissue, especially for oysters (Table III.5). Other than bivalves, only mud snails, barnacles, and mud crabs accounted for more than 1 g of nitrogen sequestered per m^2.

Table III.6. Phosphorus sequestration (g m^{-2}) by taxa from each site. Data are derived from the fauna in the incubation chambers.

Taxon	Site							
Bivalves	HM0	HMLsed	HML	HMM	HMH	1F2F	LCW	LCE
Crassostrea virginica								
Shell	0	0.626	2.286	4.831	3.9243	2.0690	0.932	0.1641
Tissue	0	0.769	1.642	4.494	2.4802	2.3294	7.2746	0.1276
Geukensia demissa								
Shell	0	0	0.005	0.023	0.0300	0	0	0
Tissue	0	0	0.021	0.076	0.0785	0	0	0
Whole organism	0	0	0.001	0.001	<0.001			
Mercenaria mercenaria							0	0
Shell	0	0.007	0.036	0.023	0.0543	0	0	0
Tissue	0	0.075	3.827	0.159	0.4968	0	0	0
Small clams (<10 mm)	<0.001	0.002	0.001	<0.001	0.0003	0	0	0
Anomia simplex	0	0.001	0.028	0	0	0	0.001	0
Gastropods								
Crepidula spp.	0	0.002	0.002	<0.001	0	0.00	0.001	0.001
Ilyanassa/mud snails	0.140	0.011	0	0	0	0.00	0	0
Crustaceans								
Amphipods	<0.001	0	<0.001	0	0.0110	<0.001	0	0.004
Barnacles	0	0.053	0.0.49	0.455	0.2042	0.010	0.001	0.009
Blue Crab	0	0.005	0.008	0	0	0.003	0	0
Hermit crab	0	0	0	0.154	0	0.00	0.00	0
Xanthid Crabs	0	0.073	0.297	0.941	1.0509	0.809	0.043	1.115
Grass Shrimp	0	0.011	0.006	0.011	0	0	0	0.176
Snapping Shrimp	0	0	0	0	0	0	0.054	0.097
Other								
Polychaetes (mostly *Alitta succinea*)	0.015	0.022	0.007	0.009	0.0230	0.004	0.0169	0.007
Molgula manhattensis	0	0.044	0.004	0.010	0.004	0	0	0.002
Gobiosoma bosci	0	0.011	0.014	0.150	0	0.048	0.048	0.189
Total	**0.155**	**1.713**	**8.231**	**11.335**	**8.357**	**5.272**	**8.375**	**1.890**

Phosphorus sequestration patterns followed those observed for nitrogen with the highest levels estimated for the HMM site and lower levels estimated for HML, HMH and LCW (Table III.6). Importantly, even the two reef sites with the lowest phosphorus sequestration (HMLsed and LCE) had an order of magnitude more phosphorus sequestered in macrofaunal biomass than did the site without oysters (HM0).

III-4 Flux measurements

Flux measurements were made in all of the chambers under light and dark conditions to distinguish between the roles of autotrophs and heterotrophs in the movement of materials between the water column and the benthos. By convention, fluxes of materials from the water column to the bottom are given negative values and fluxes from the bottom into the water column are given positive ones.

Oxygen Flux - Oxygen fluxes in chambers from all stations were negative, indicating uptake of O_2 within the bottom, largely a result of respiration by benthic organisms (Fig. III.2). Oxygen production through photosynthesis in the chambers, which can be computed as the difference between fluxes under light and dark conditions, was small relative to benthic respiration. Photosynthetic rates of ~500 to 2,500 $\mu mol\ O_2\ m^{-2}\ h^{-1}$ are similar to those observed in other Chesapeake Bay shallow water environments (Reay et al. 1995; Chick 2009).
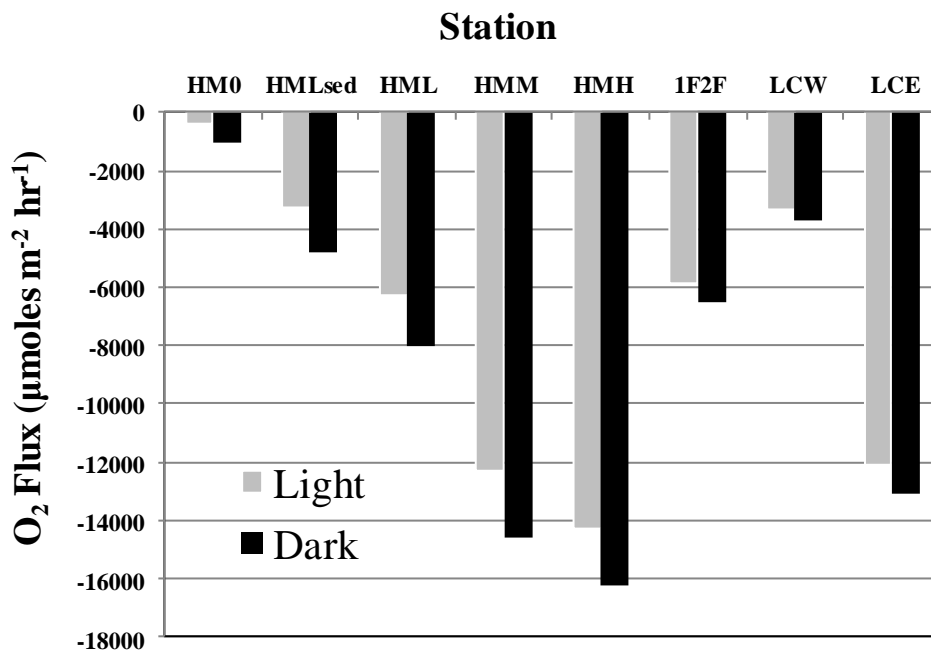

Figure III.2. Oxygen flux under light and dark conditions in incubation chambers from each station. Station codes are as in Table II.1. Negative values represent fluxes from the water column to the benthos.

Oxygen consumption in the Humes Marsh treatments increased monotonically with oyster abundance and biomass measurements made at the field sites (compare values in Table III.1 to Humes Marsh treatments in Fig. III.2). There is not a similar clear relationship between the other three stations, where the Long Creek East treatment had much higher fluxes than the other two sites, despite having similar oyster abundances and biomass.

When we plot the same oxygen consumption data against the soft-tissue biomass of macrobenthic organisms found in each incubation chamber, there is no clear relationship (Fig. III.3). However, when oxygen consumption is plotted against total biomass, including shells of living bivalves, a positive relationship between macrobenthic biomass and oxygen uptake is evident, with the exception of a single outlier (Fig. III.4). The outlier in this case is from the Long Creek East site, which as we will see later is anomalous in several ways. Removing this outlier reveals linear relationships between oxygen uptake and total macrobenthic organism (including shells from living bivalves) under both light and dark conditions (Fig. III.5).
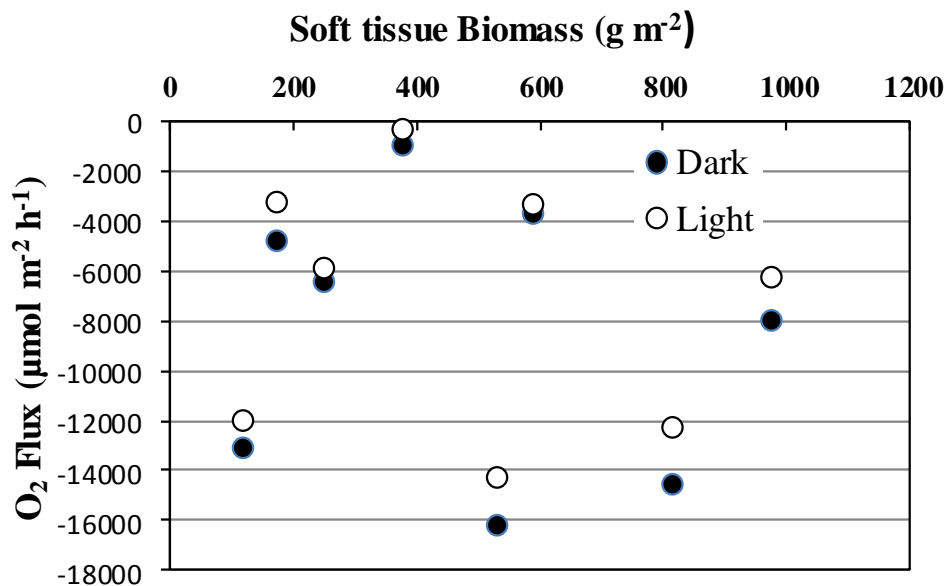

Figure III.3. Oxygen flux under light and dark conditions in relation to soft tissue biomass of macrobenthic organisms (including oysters) in the incubation chambers.
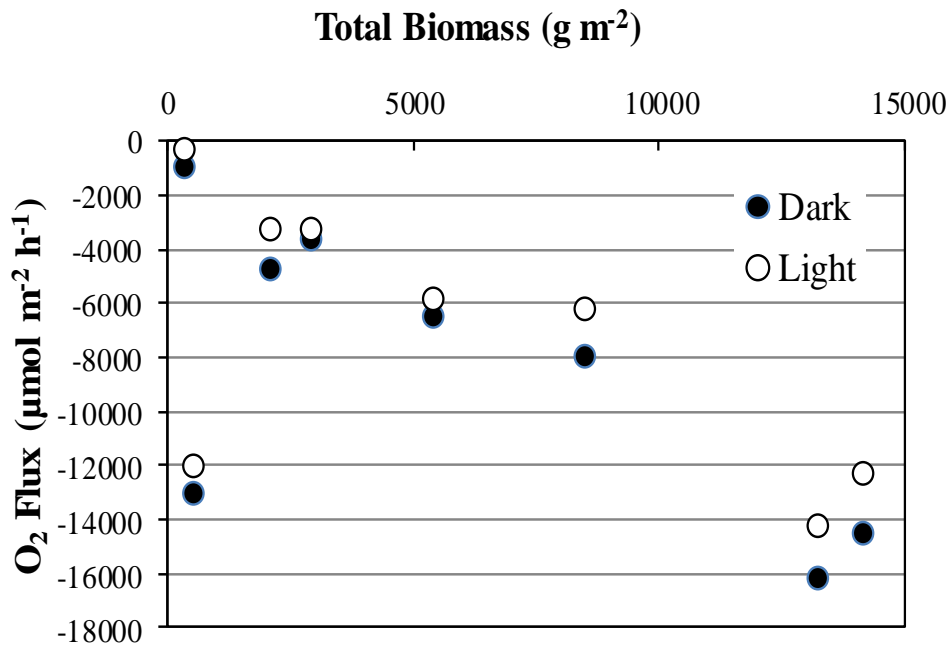
Figure III.4. Oxygen flux under light and dark conditions in relation to total biomass of macrobenthic organisms in incubation chambers, inclusive of shells from live bivalves.

Figure III.5. Oxygen flux under light and dark conditions in relation to total biomass of macrobenthic organisms in incubation chambers, inclusive of shells from live bivalves and excluding the LCE site.
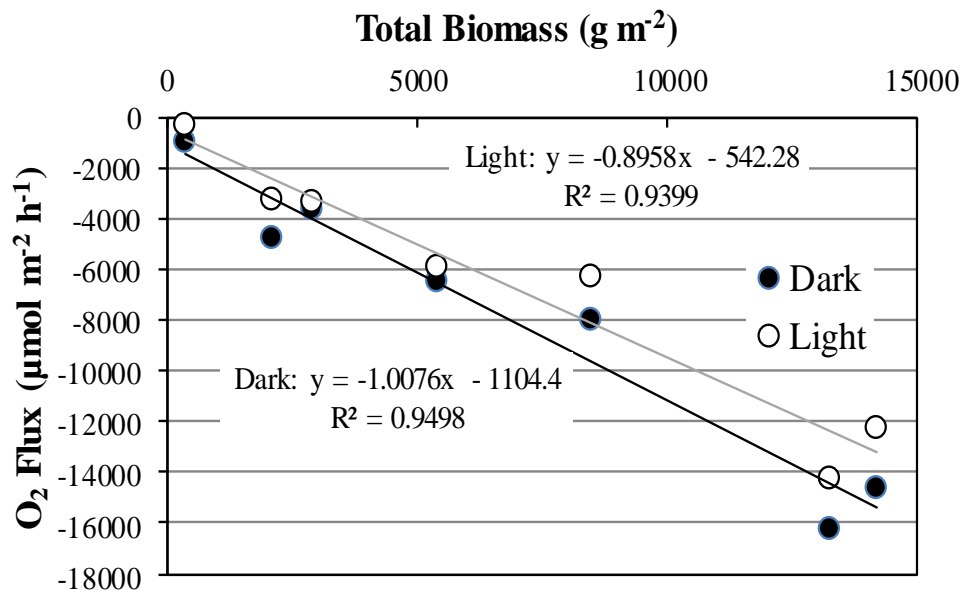
25

Ammonium nitrogen flux – Fluxes of nitrogen in the form of ammonium from the water column to the benthos (negative fluxes) reflect uptake by macro- and micro-benthic algae. Release of ammonium from the benthos into the water column reflects both direct release by oysters and other macrofauna and remineralization of more complex organic nitrogen biodeposits by microbes (see Fig. I.1). Uptake of ammonium by the benthos was observed in only three of the incubation chambers under light conditions (Fig. III.6). The two site at Humes Marsh with a soft sediment base and the Long Creek West site, which also lacked a shell base, were observed to uptake NH_4^+ at rates between 103 and 288 µmoles m^{-2} hr^{-1} (Fig. III.6). The highest rates observed here (> 1,000 µmoles m^{-2} hr^{-1}) are higher than observed rates under anoxic conditions in the Chesapeake mid-bay region (Cowan and Boynton 1996) but lower than summer rates in the Choptank River (Kellogg et al. 2011).
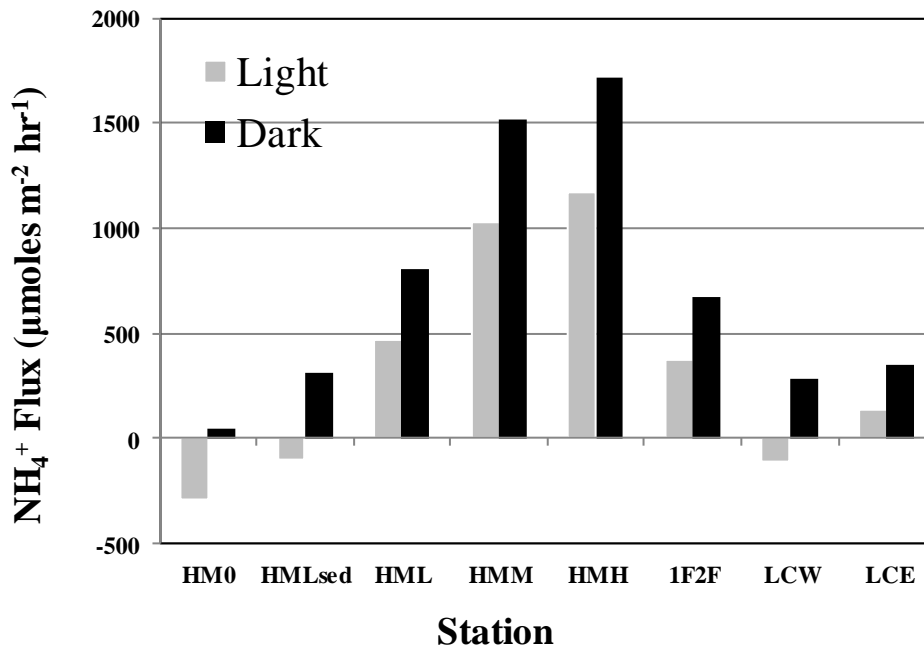

Figure III.6. Ammonium (NH_4^+) flux under light and dark conditions in incubation chambers from each station. Negative values represent fluxes from the water column to the benthos.

There is a weak positive relationship between ammonium flux and soft-tissue biomass, inclusive of oysters, in the incubation chambers from each site (Fig. III.7). This relationship, however, is much stronger when the biomass estimates include the shell from live bivalves within the chambers, with over 90% and 94% of the variation in NH_4^+ measurements in light and dark conditions, respectively, explained by the total macrofauna biomass within the chambers (Fig. III.8). Interestingly, comparably good relationships were observed between ammonium flux and the soft-tissue biomass from oysters measured at the field sites at the time chamber base trays were deployed (Fig. III.9).
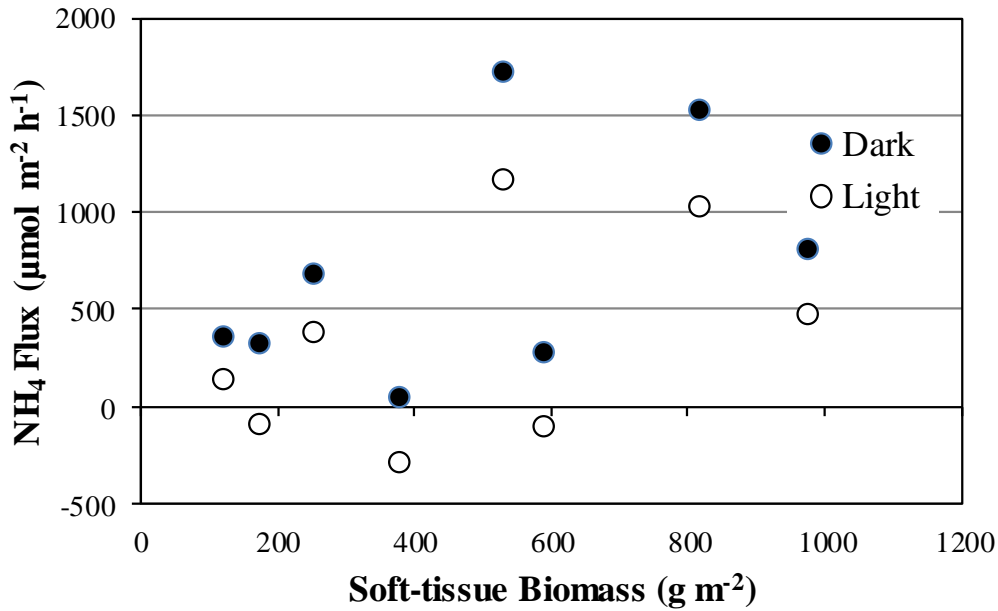
Figure III.7. Ammonium (NH_4^+) flux under light and dark conditions in relation to soft-tissue biomass (including oysters) in the incubation chambers.
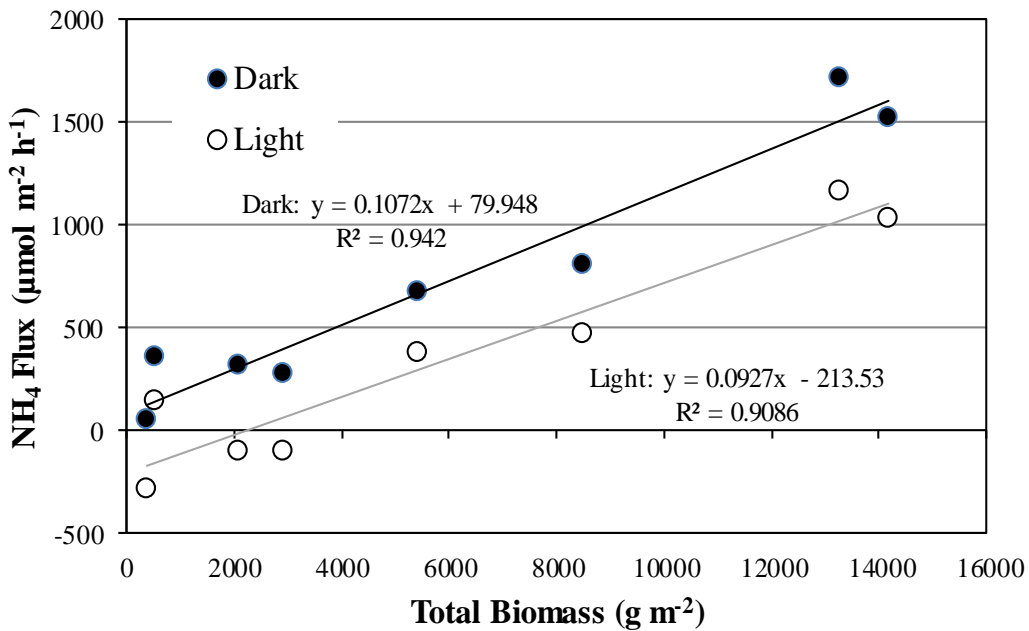

Figure III.8. Ammonium (NH_4^+) flux under light and dark conditions in relation to total biomass in incubation chambers, inclusive of shells from live bivalves.
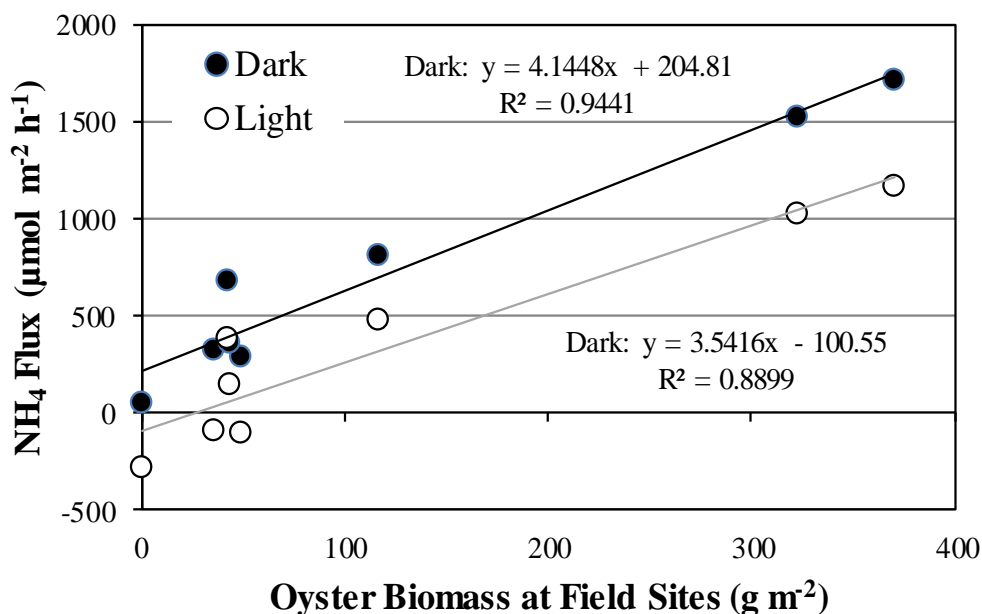
Figure III.9. Ammonium (NH_4^+) flux under light and dark conditions in relation to oyster soft-tissue biomass at the field collection sites

NO2 and NO3 nitrogen flux – Nitrite (NO_2) and nitrate (NO_3) flux from the benthos into the water column is largely a consequence of the remineralization of organic nitrogen by sediment microbes (with nitrification of the ammonium producing NO_2 and NO_3; see Fig. I.1). As with ammonium, this flux has the potential to drive phytoplankton growth. Fluxes from the water column to the benthos are largely the result of uptake by benthic macro- and micro-algae, although under dark conditions diffusion into nitrate-reducing sediment zones is likely. The analytical method that we used did not distinguish between NO_2 and NO_3, and therefore we use the shorthand convention NO_{2+3} to refer to the total of these two compounds.

Observed NO_{2+3} fluxes in our experiment were positive in all cases except the Humes Marsh site without oysters or shell (Fig. III.10). The NO_{2+3} flux rates measured for the Long Creek East site were 849 µmoles m^{-2} hr^{-1} under light conditions and 960 µmoles m^{-2} hr^{-1} under dark conditions. This greatly exceeded the rates observed at the other sites where rates ranged from -20 to 219 µmoles m^{-2} hr^{-1} (Fig. III.10).
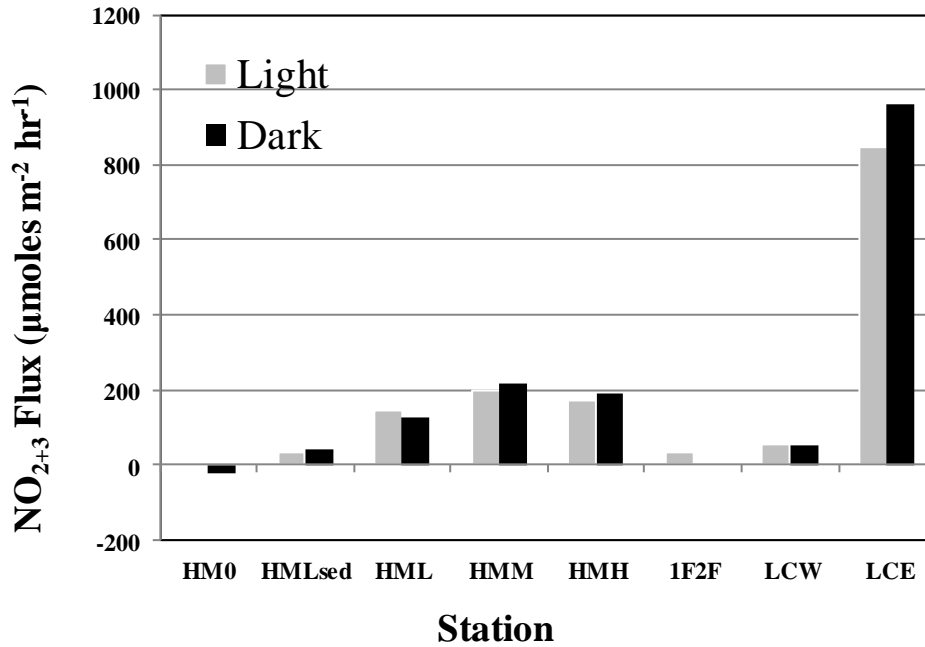
Figure III.10. NO_{2+3} flux under light and dark conditions in incubation chambers from each station.

The observed high values for NO_{2+3} at the LCE site are not related to the soft-tissue biomass of macrobenthic organisms (Fig. III.11).   A weakly positive relationship between soft-tissue biomass within the chambers and NO_{2+3} is observed for the other stations, but not for LCE. When data for that outlier site are removed and NO_{2+3} flux is plotted against total macrofauna biomass (including the shells of live bivalves), strong positive relationships are observed under both light and dark conditions (Fig. III.12).

.

Figure III.11. Nitrite and nitrate (NO_{2+3}) flux under light and dark conditions in relation to soft-tissue biomass of macrobenthic organisms in incubation chambers. The LCE site is an obvious outlier.
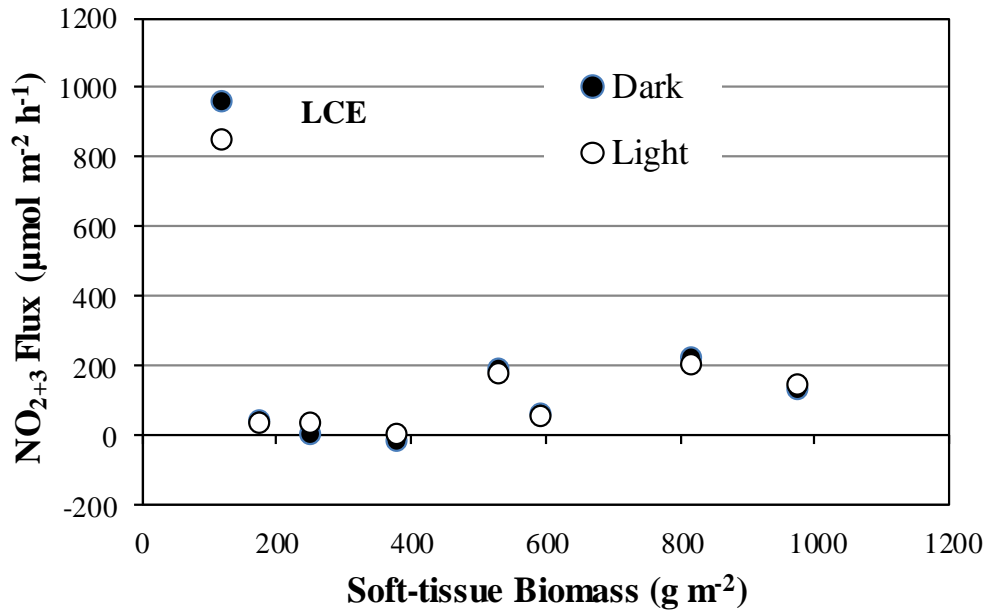

Figure III.12. Nitrite and nitrate (NO_{2+3}) flux under light and dark conditions in relation to total biomass (including shells of live bivalves) in incubation chambers. Data from LCE site has been removed.

Di-nitrogen nitrogen flux – Flux of di-nitrogen (N_2) from the sediments into the water column results largely from microbially mediated denitrification in anoxic sediments (see Fig. I.1). High rates of di-nitrogen flux require a large source of NO_{2+3}; at these sites, low rates of NO_{2+3} uptake suggest nitrification is the source. Once in the water column, N_2 gas will diffuse into the atmosphere, effectively removing the nitrogen from the aquatic environment.

N_2 flux rates ranged from a non-detectable flux at HMLsed in the dark to 324 μmoles m^{-2} hr^{-1} in the dark at LCE (Fig. III.13). There was not a consistent pattern in flux rate between light and dark conditions, but the sites with shell bases (HML, HMM, HMH, and LCE) generally had higher flux rates than those in sedimentary habitats. The subtidal site in Long Creek with a shell base, LCE, had the highest rates of N_2 flux among all of the stations, despite the fact that neither the oyster density and biomass at the site (Table III.1) nor the macrofaunal density and biomass within the incubation chambers (Tables III.2 and III.3) were among the highest within the study. Plots of N_2 flux versus total soft-tissue biomass of macrobenthic organisms in the chambers (Fig. III.14), total biomass (including the shells of live bivalves) within the chambers (Fig. III.15), and oyster biomass at the field site (Fig. III.16) all reveal site LCE to be an outlier, with high N_2 values and low biomass values.
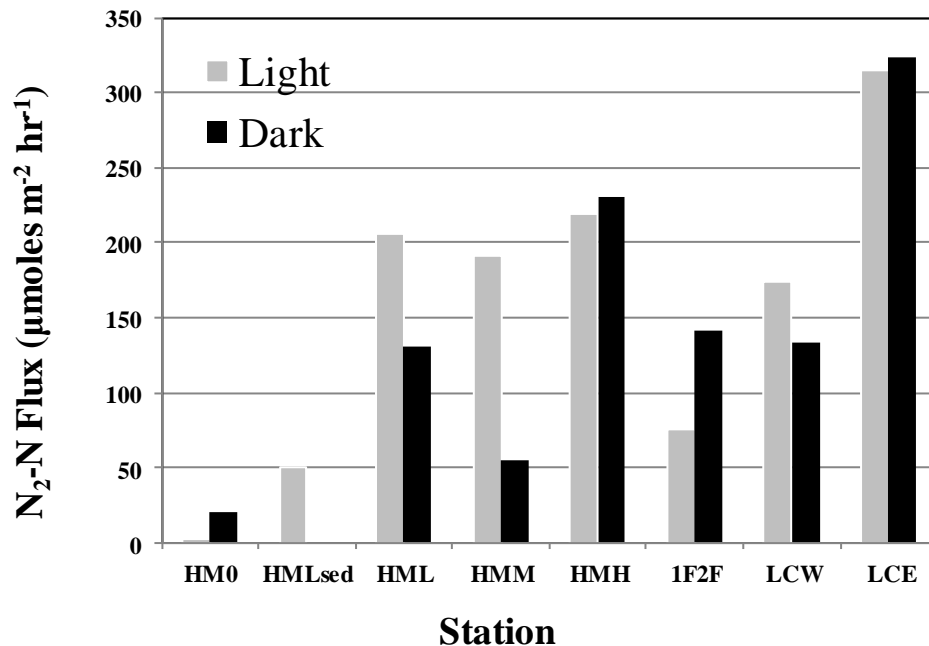
Figure III.13. N_2 nitrogen flux under light and dark conditions in incubation chambers from each station.
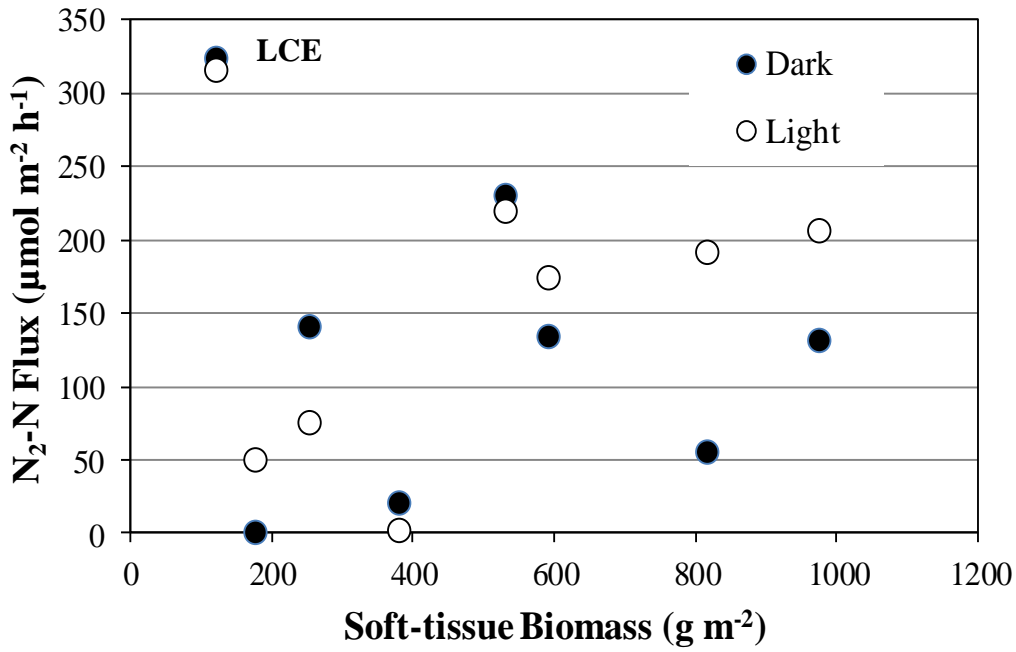
Figure III.14. N_2 flux under light and dark conditions in relation to total soft-tissue biomass of macrobenthic organisms in incubation chambers. The LCE site is an obvious outlier.
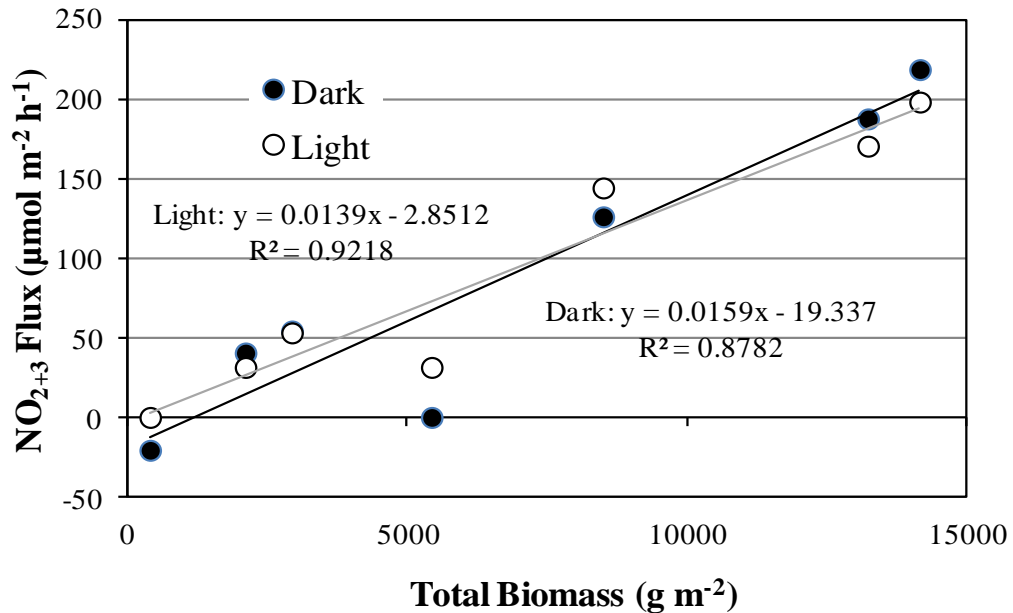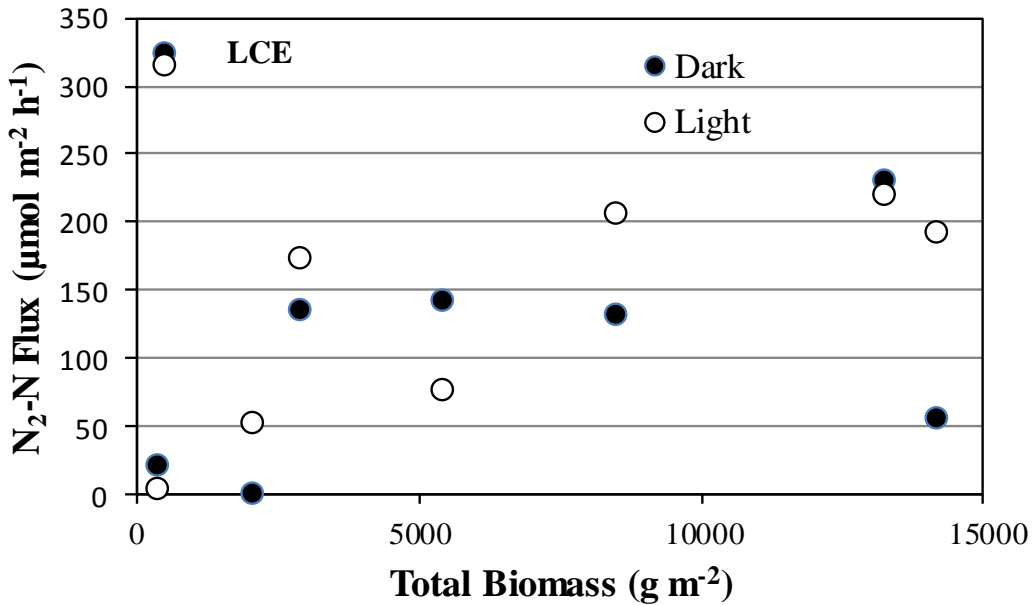

Figure III.15. N_2 flux under light and dark conditions in relation to total biomass (including shells of live bivalves) within incubation chambers. The LCE site is an obvious outlier.
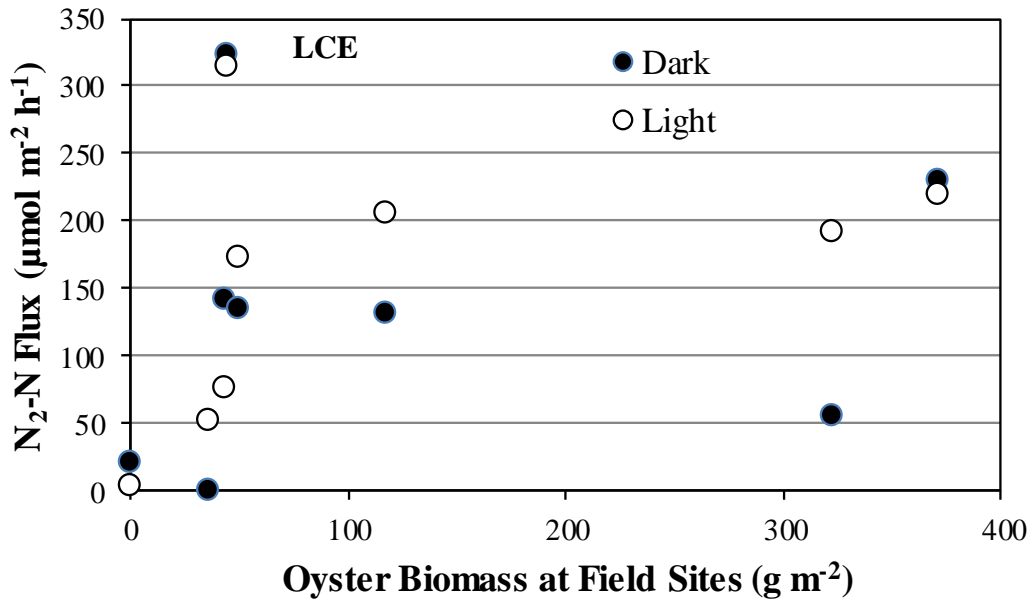
Figure III.16. N_2 flux under light and dark conditions in relation to oyster soft-tissue biomass at the field collection site. The LCE site is an obvious outlier.

Total nitrogen flux – Total measured nitrogen fluxes under both light and dark conditions reveal differences in magnitude and composition between stations (Figs. III.17 and III.18).

Figure III.17. Total nitrogen flux under light conditions at each station by nitrogen species.

Figure III.18. Total nitrogen flux under dark conditions at each station by nitrogen species.

Under both light and dark conditions there is a clear positive relationship between total nitrogen flux and oyster abundance and biomass at the intertidal Humes Marsh sites, the majority of which is NH_4^+ flux. NO_{2+3}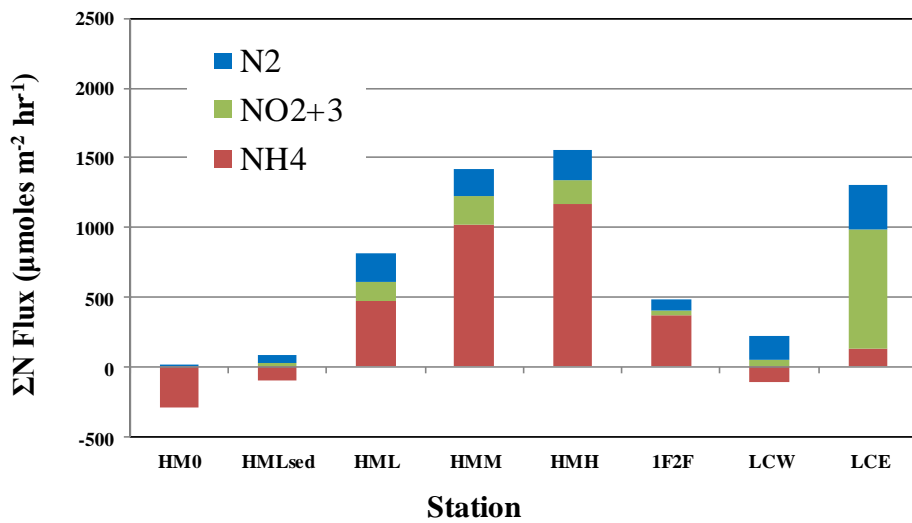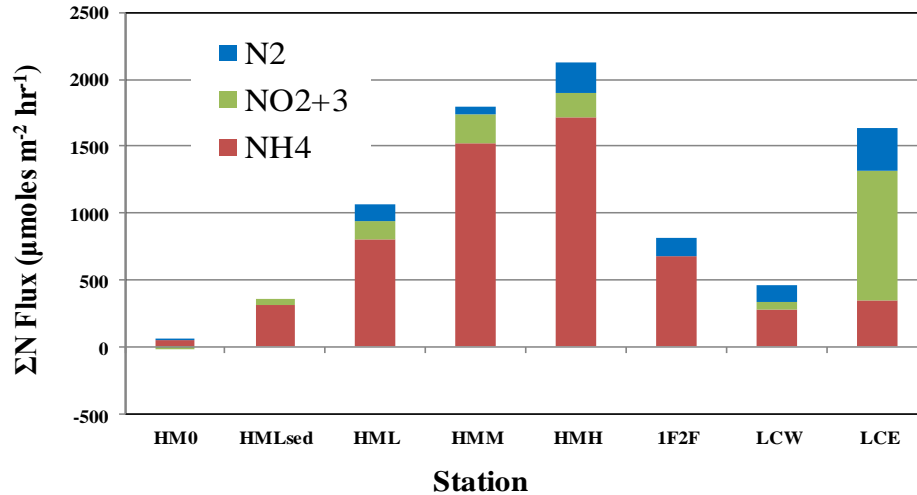 and N_2 flux comprise about 20% of the nitrogen flux measured for the Humes Marsh stations with oysters. The 1F2F station had a similar pattern with NH_4^+ accounting for about 80% of the observed nitrogen flux (Figs. III.17 & III.18). The very small proportion of NO_{2+3} flux measured in the chamber from this site indicates that the products of nitrification are rapidly denitrified to form N_2. At the subtidal LCW site higher proportions of nitrogen underwent nitrification (NO_{2+3} + N_2 flux) and denitrification (N_2) than at the intertidal sites. Most of the nitrogen flux observed at the other subtidal site, LCE, was in the form of NO_{2+3}. The lower proportions of NH_4^+ and N_2 along with the higher proportion of NO_{2+3} at this site indicate that much of the ammonium is undergoing nitrification, but that a relatively small proportion of the NO_{2+3} is undergoing denitrification.

Nitrification and denitrification efficiency – Nitrification is the source of both nitrite and nitrate (NO_{2+3}) efflux to the water and NO_{2+3} available for denitrification. Nitrification efficiency is expressed as the percentage of total inorganic nitrogen flux that is converted to NO_{2+3}:

$$\% \text{ Nitrification Efficiency} = \frac{(N_2\text{-}N) + (NO_{2+3})}{\Sigma N} \times 100$$

where: N_2-N = di-nitrogen flux
   ΣN = total inorganic nitrogen flux.

Plotted as percent nitrogen flux, nitrification efficiencies at the sites with oysters ranged from 11% to 78% of total nitrogen (Fig. III.19). The lack of a value for nitrification efficiency at the control site without oysters (HM0) results from the fact that at this site there was a net uptake of NO_{2+3} by the sediments (see Fig. III.10).

Denitrification efficiency is a measure of how efficiently nitrogen is processed into forms that are unavailable to algae for growth. It can be expressed as:

$$\% \text{ Denitrification Efficiency} = \frac{N_2\text{-}N}{\Sigma N} \times 100$$

where: N_2-N = di-nitrogen flux = denitrification
ΣN = total inorganic nitrogen flux = sum of NH_4^+, NO_{2+3}, and N_2-N fluxes.

Percent denitrification observed for oyster reef sites in this study ranged from undetectable at HMLsed to nearly 30% of total inorganic nitrogen flux at the LCW (Fig. III.19).
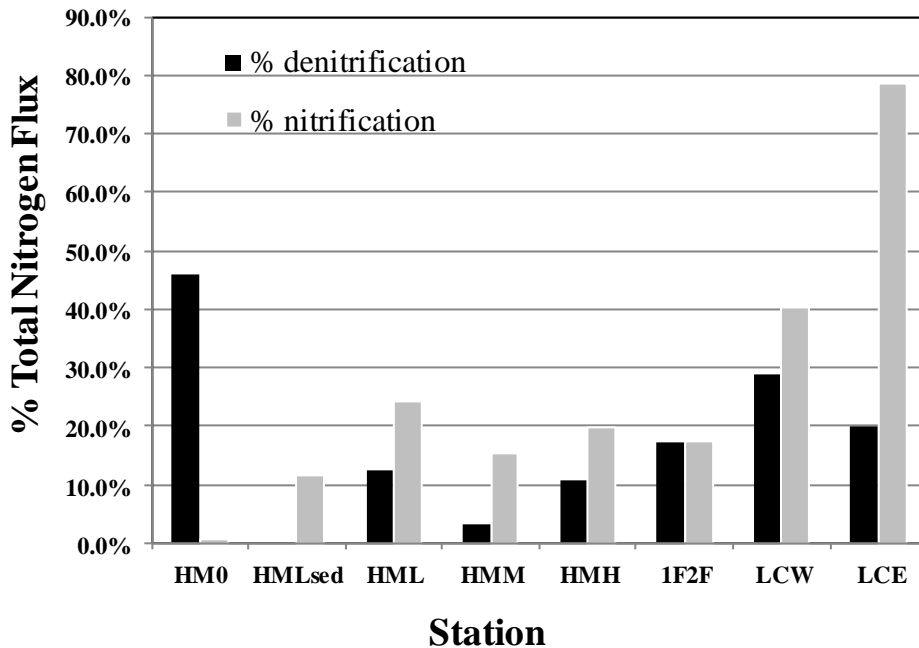

Figure III.19. Percentages of total inorganic nitrogen flux attributable to nitrification and denitrification in incubation chambers from each station.

Nitrogen flux stoichiometry – We can use basic stoichiometry (chemical balance equations) as a check on our measured nitrogen flux rates. The Redfield ratio provides an empirically determined stoichiometric relationship between C:N:P of 106:16:1. Direct measurements of carbon flux on an oyster reef are unlikely to correspond to the Redfield ratio because carbon fluxes occur in association with the production and dissolution of calcium carbonate as well as in association with the breakdown of organic matter. Since respiration involves the uptake of two O molecules for each C molecule, we can use O_2 as a 1:1 proxy for carbon flux from respiration. Plotting our measured total nitrogen fluxes against measured O_2 fluxes demonstrates a tight relationship between carbon and nitrogen flux indicating that our measurements of both fluxes are reasonable (Fig. III.20), The position of these data points 15-20% below the Redfield ratio line is potentially indicative of nitrogen sequestration.
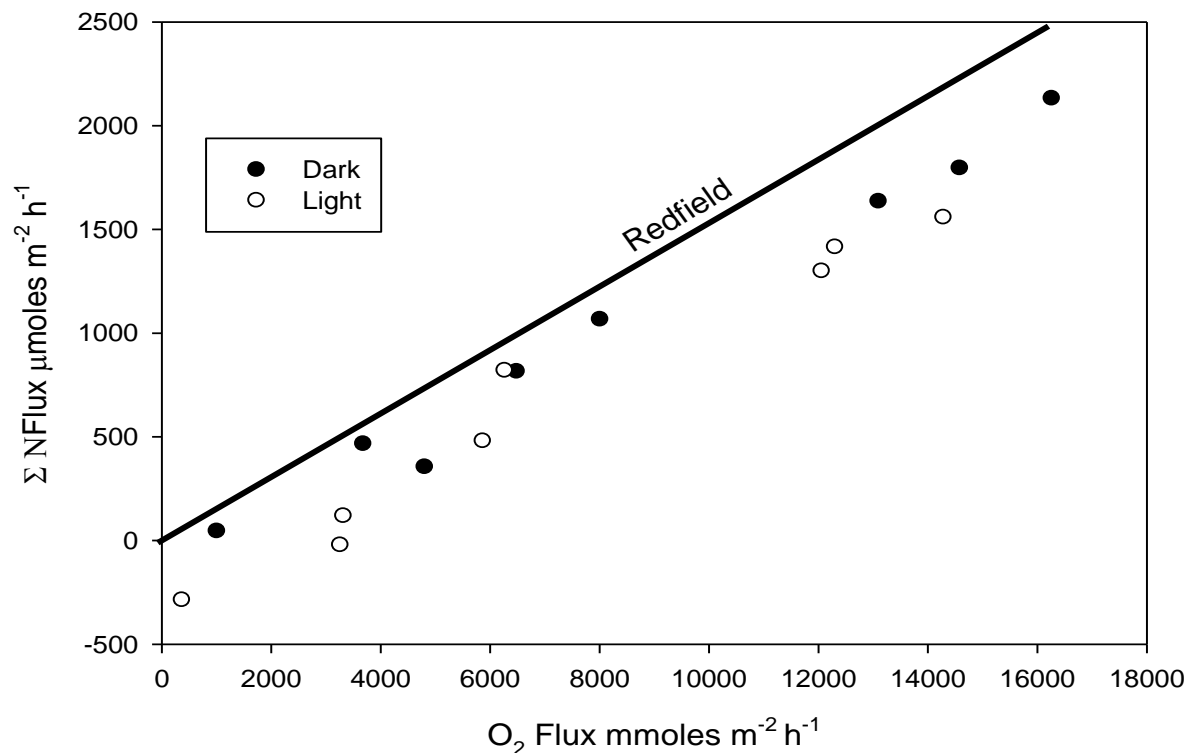
Figure III.20. Relationship between oxygen flux and total nitrogen flux under light and dark conditions in the incubation chambers from each station. The solid line represents stoichiometry from the Redfield ratio.

Soluble reactive phosphorus flux – Fluxes of soluble reactive phosphorus (SRP) were highly variable across sites in this study, ranging from -52 to 28 μmoles m^{-2} hr^{-1} (Fig. III.21). In the dark, all observed fluxes represent uptake by the benthos from the water column. Under light conditions, SRP uptake was observed at the HML, 1F2F and LCE sites, while release from the benthos into the water column was observed at the HMM and HMH sites (Fig. III.21). These results are in stark contrast to SRP fluxes from a restored reef in the Choptank River where measure fluxes were higher and stoichiometrically balanced relative to O_2 and to ΣN fluxes (Kellogg et al. 2011) - there was no significant reduction of phosphorus from the water column caused by the presence of oyster reefs at sampled sites in the Lynnhaven.
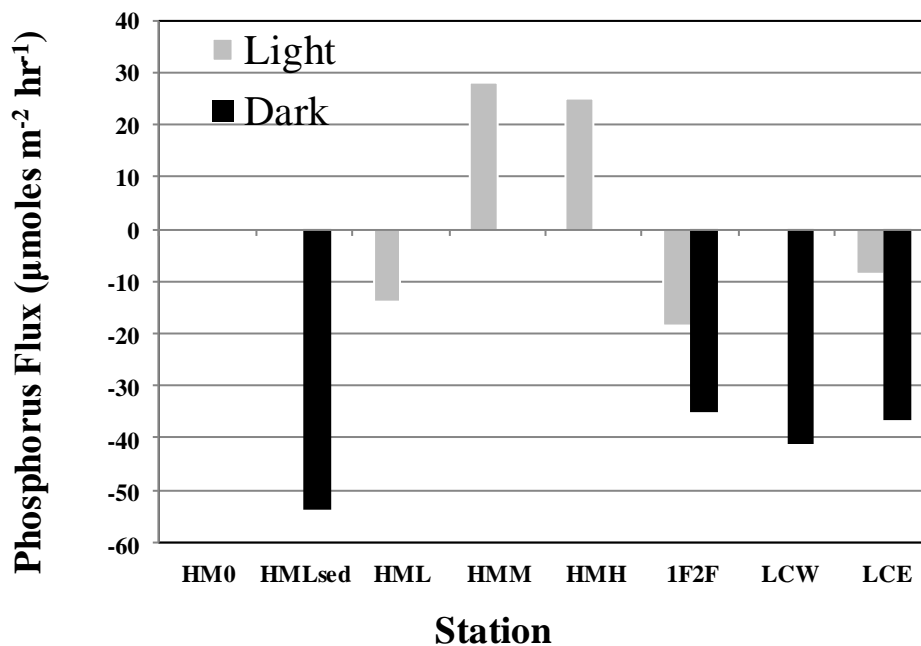
Figure III.21. Soluble reactive phosphorus flux under light and dark conditions in incubation chambers from each station. Negative values represent fluxes from the water column to the benthos.

III-5 Biomass-Specific Oyster Filtration and Biodeposition Rates

The first element of this section involved calculation of the relationship between oyster mass (ash-free dry mass, AFDM) in g and shell height (SH) in mm specifically for the Lynnhaven River system (Fig. III.22). Lab processing included counts of oysters, and measurement of SH. Dry mass (DM), ash free dry mass (AFDM), and condition index (CI) were calculated for selected oysters. A subsample of oysters collected throughout the range of oyster shell heights was processed by removing fouling organisms and rinsing. After cleaning, oysters were blotted dry before being measured. Measurements made on each oyster included total mass (nearest 0.001 g), SH (nearest 0.1 mm), and wet shell mass (nearest 0.001 g). After shucking, shells and tissue were dried at 60°C for at least 48 h and weighed (DM), followed by 6 h at 550°C in a muffle furnace to account for the ash in DM and produce AFDM estimates.
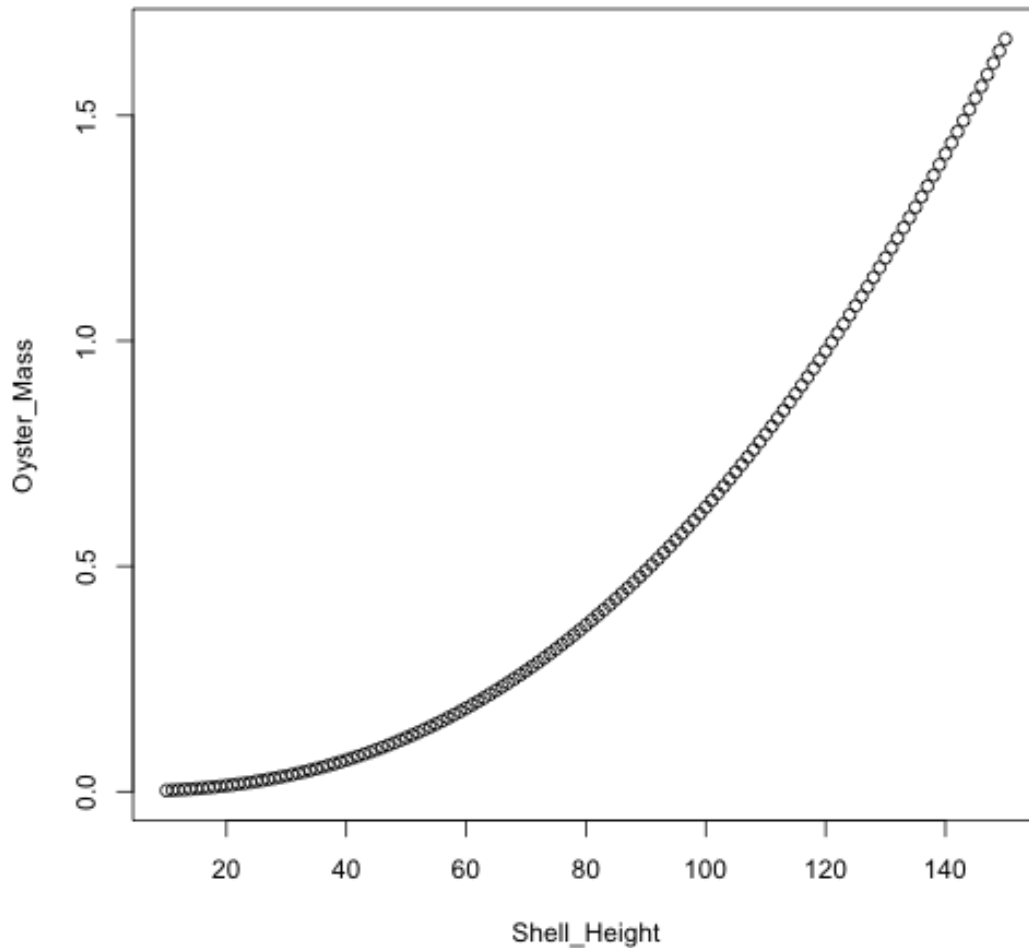
Figure III.22. Relationship between oyster shell height and dry mass (Oyster Mass = $0.00001(SH^{2.4})$) as adapted from Burke (2010).

This function can be used as a standard for comparison with studies in other locations to generate the expected weight of oysters of different sizes when determining biomass-specific filtration and biodeposition rates.

Next we analyzed the relationship between Biodeposition Rate in (mg of sediment) (g dw of oyster)$^{-1}$ hour^{-1} and Total Suspended Solids (TSS) in mg L^{-1}, as derived from the Jordan (1987) data set. We initially conducted the statistical analyses exactly as done in Jordan (1987), by analyzing log-10 of Biodeposition Rate as a function of Temperature and Seston Concentration, using various combinations of the two independent variables in polynomial functions. Salinity was excluded from the analysis because it was not a significant variable in the analyses of Jordan (1987). Examination of the diagnostic measures for the analysis using temperature and seston concentration indicated that there were serious deviations from the statistical assumptions underlying regression analysis, including non-random residuals

(Fig. III.23), excessively non-normal residuals, and non-random residuals with a high leverage (influence) upon the regression model (Fig. III.24).

Figure III.23. Plot of residuals against the fitted values of the regression.
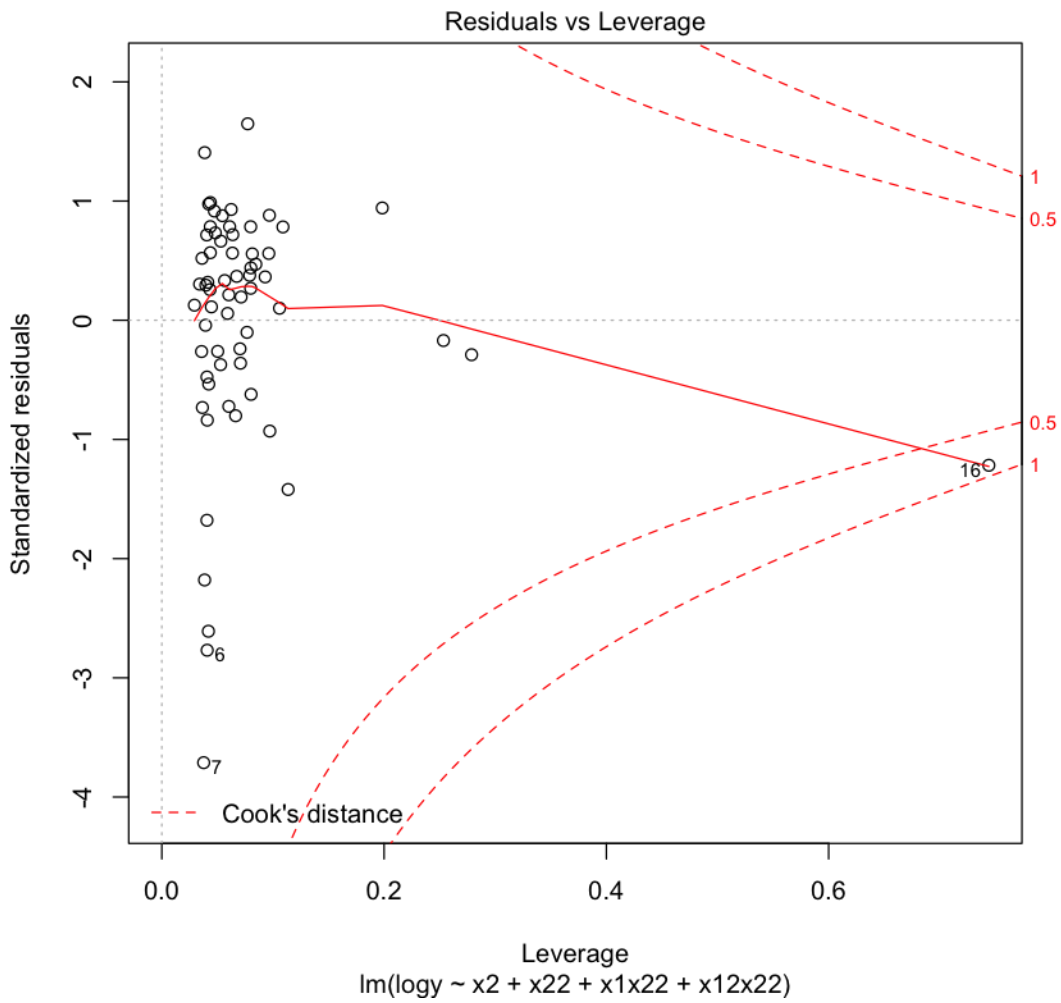
Figure III.24. Non-random residuals with their leverage scores (influence upon the regression model).

Given the poor fit of the biodeposition data in the previous analysis, we analyzed the Biodeposition data as a function of Seston concentration (Fig. III.25) and Water Temperature (Fig. III.26) with non-linear regression.

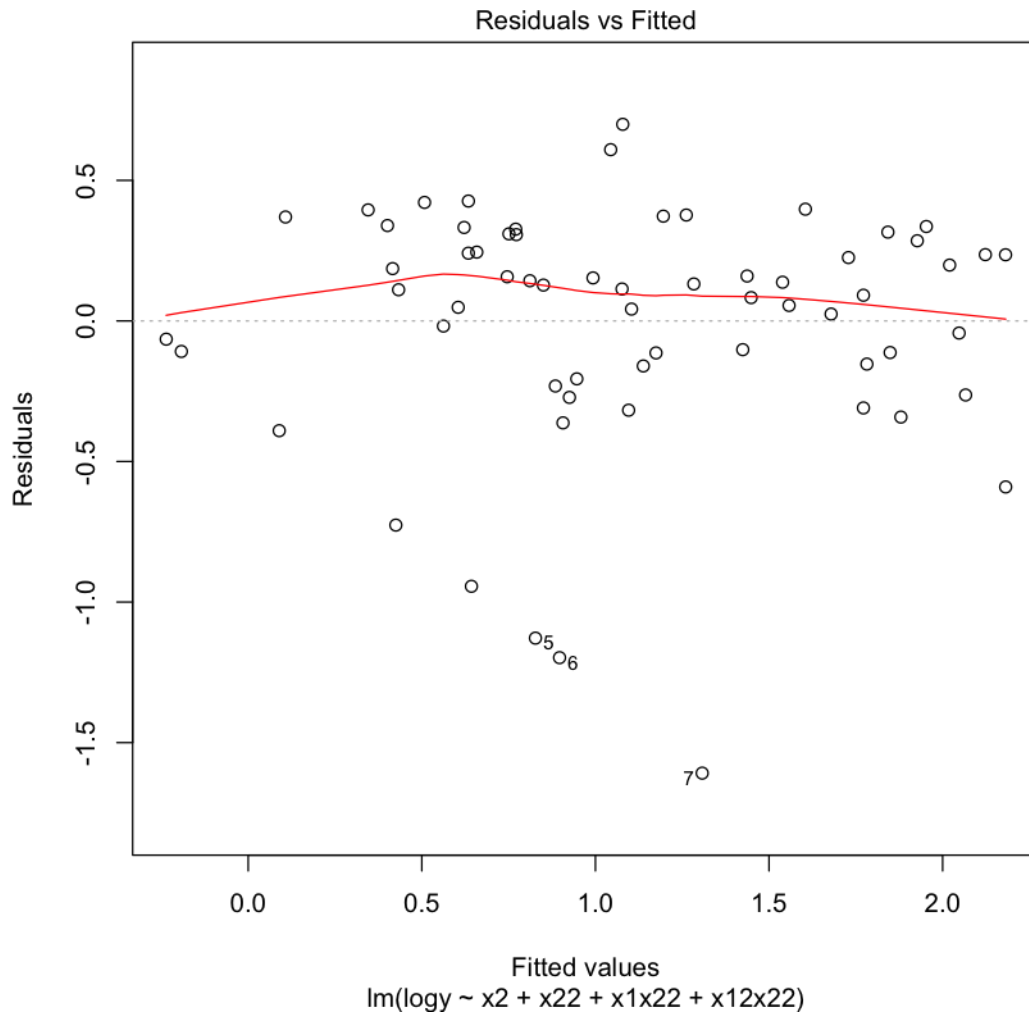For biodeposition (and thus filtration), the relationship between Biodeposition Rate and Seston concentration was a Ricker function with strong density dependence (Allee effect) at low TSS values (Fig. III.25). This indicates that at very low levels of seston concentration, oysters cease filtering, most likely due to the poor benefit:cost metabolic ratio at low seston concentrations. Specifically, oysters will expend more energy filter feeding at low seston concentrations than they receive from the filtered material. In contrast, at high seston concentrations biodeposition rates were low due to an inability of oysters to filter effectively at high seston concentrations, such that their filtration apparatus becomes clogged with sediment particles and shuts down. Note that filtration is density-dependent (= depensatory) at low TSS, and negatively density-dependent (= compensatory) at high TSS.
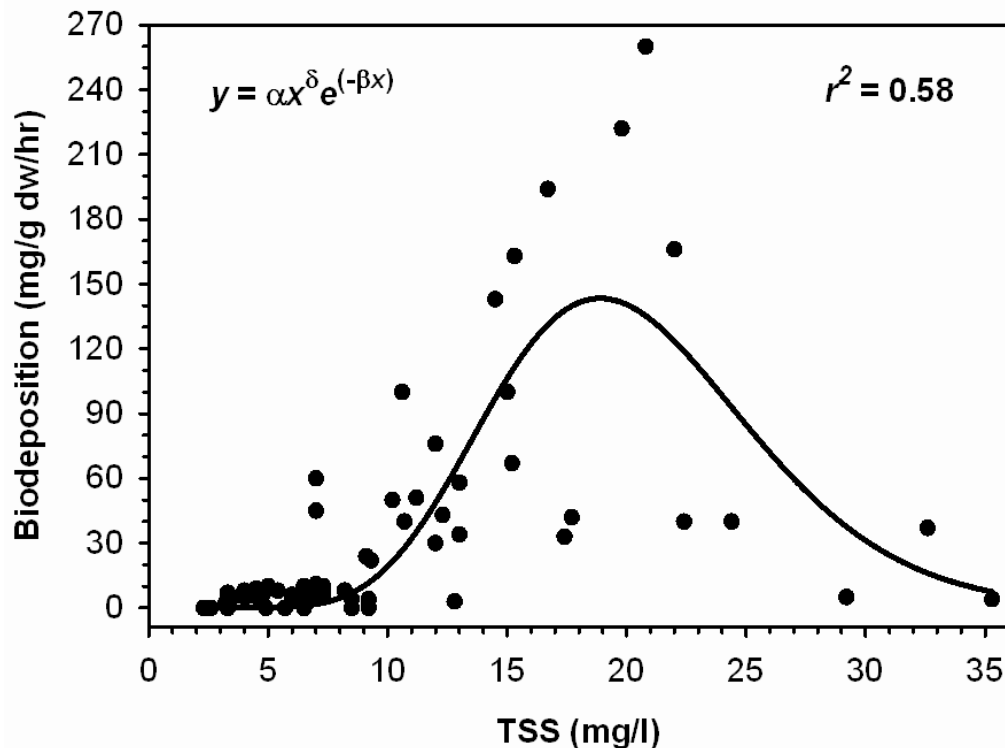
Figure III.25. Biodeposition rates as a function of Seston concentration. The parameter estimates are: $\alpha = 0.000000009$ (sets maximum), $\beta = 0.64$ (shape parameter), $\delta = 12.14$ (depensation parameter).

Next we analyzed Biodeposition Rate as a function of Water Temperature, and found a significant positive relationship (Fig. III.26). This relationship was expected given the generally positive relationship between metabolic rates and temperature. Note also that variance increased with temperature. As physiological rates and other metabolic processes

increase with temperature, so does their variability. This is a typical response, and results from the fact that the variance of a variable usually scales with its mean.
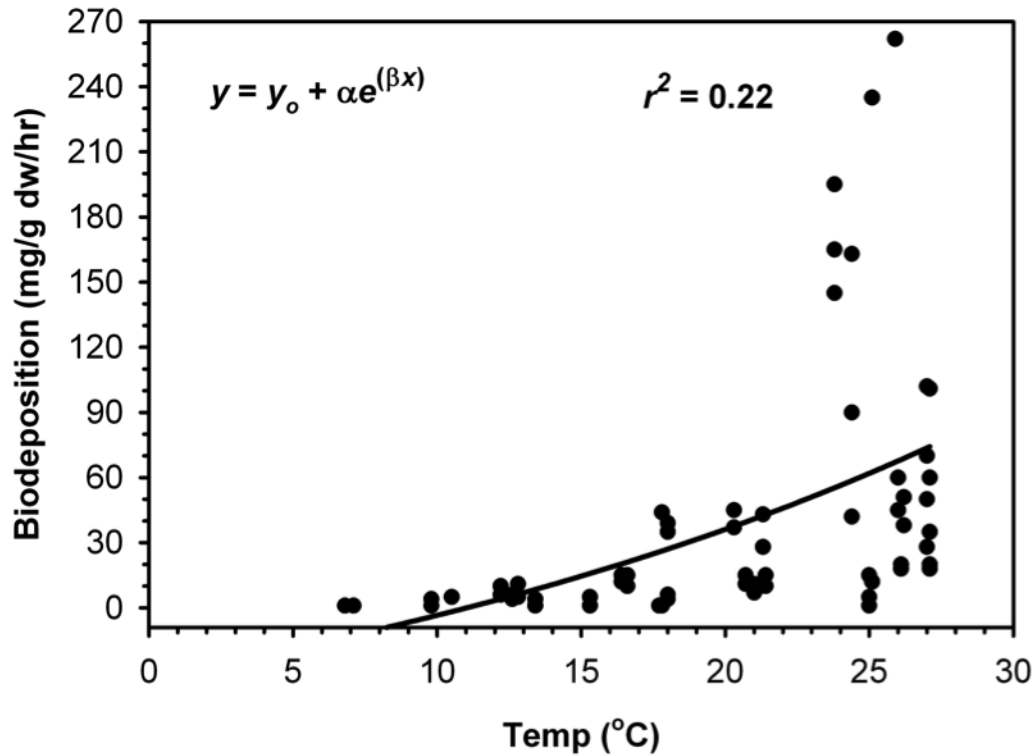
Figure III.26. Relationship between Biodeposition Rate and Water Temperature. The parameter estimates are: y_0 = -95.22, α = 64.14, and β = 0.04.

Note that the two analyses were conducted independent of one another, such that the modeling of biodeposition rate did not account for the synergistic effects of the two independent variables (seston concentration and water temperature) on biodeposition rate. From these two analyses, we conclude that the final equation used in the hydrodynamic model has to be based on both water temperature and seston concentration in a non-linear predictive model.

The model chosen incorporates the joint effects of water temperature and seston concentration on biodeposition, as well as the fundamental aspects of the relationships between filtration, temperature and seston concentration. Specifically, the model accounts for (i) a threshold effect of low seston concentration upon filtration, (ii) a clogging effect of high seston concentration upon filtration, and (iii) a positive correlation between filtration and temperature. The specific mathematical model is as follows:

$$BD = (\alpha \times T) \times (TSS^{\beta}) \times e^{-\delta \times TSS}$$

where BD = biodeposition rate (mg per g DW per hr),

  T = water temperature (^{o}C),

  TSS = seston concentration (mg per L),

  α = a parameter that determines peak biodeposition rate proportional to temperature,

  β = a parameter that determines both peak biodeposition rate and the position of the peak as a positive function of seston concentration, and

  δ = a parameter that determines both peak biodeposition rate and the position of the peak as an inverse function of seston concentration.

We conducted a non-linear regression using this model, which detemined that the following equation relates biodeposition rate to seston concentration and temperature, with an approximate r^2 = 0.64 (Fig. III.27):

$$BD = (0.00000000 \mathrm{l} \times T) \times (TSS^{10.377}) \times e^{-0.54 \times TSS}$$

Note that the model accounts for the three key characteristics of filtration: (i) a threshold effect of low seston concentration upon filtration, whereby filtration and biodeposition become negligible at seston concentrations below about 5-10 mg/L, (ii) a clogging effect upon filtration at high seston concentrations greater than 20 mg/L, and (iii) a positive correlation between filtration and temperature, with filtration rate decreasing from a high at 25-30°C to a low at 5oC (Fig. III.27).

We then converted the biodeposition rate to filtration rate by dividing the biodeposition rate by seston concentration (Jordan 1987), and then multiplying by 8 to calibrate filtration rate to a level of approximately 7 L h^{-1} at 25°C, which matches mesocosm observations (Newell and Koch 2004). The final equation for filtration rate is (Fig. III.28):

$$CR = \frac{\left((0.0000000 8 \times T) \times (TSS^{10.377}) \times e^{-0.54 \times TSS}\right)}{TSS}$$

where CR = filtration rate (L per g DW per hr).

Note that biodeposition and biofiltration are positively related to oyster weight, such that water quality measures need not account for oyster reef height, but only oyster biomass as determined from oyster reef and habitat surveys.

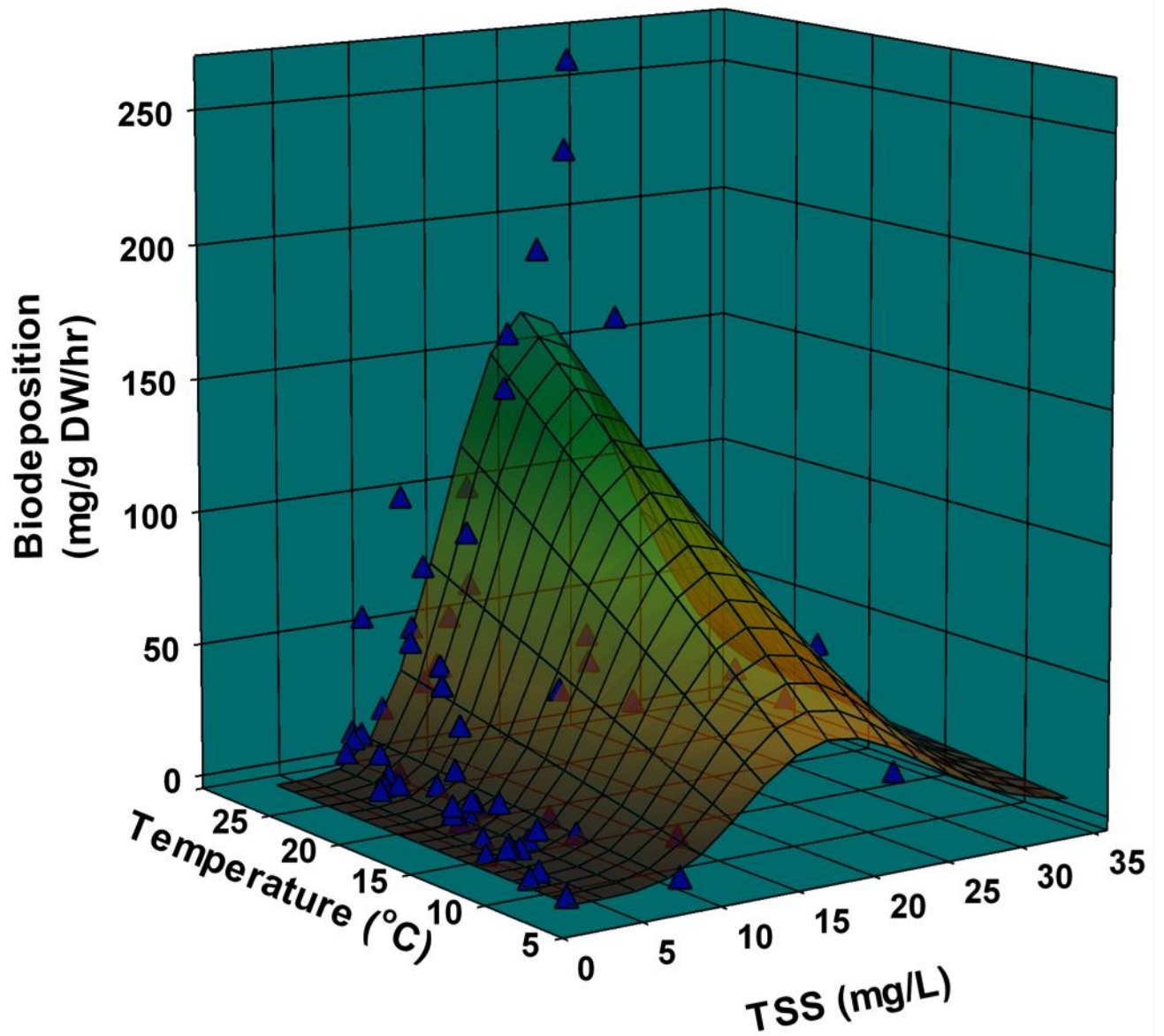Figure III.27. Mesh plot of the function relating biodeposition rate to seston concentration and water temperature. The data points are actual observations from Jordan (1987), while the mesh plot is derived from the equation relating biodeposition rate to water temperature and seston concentration.
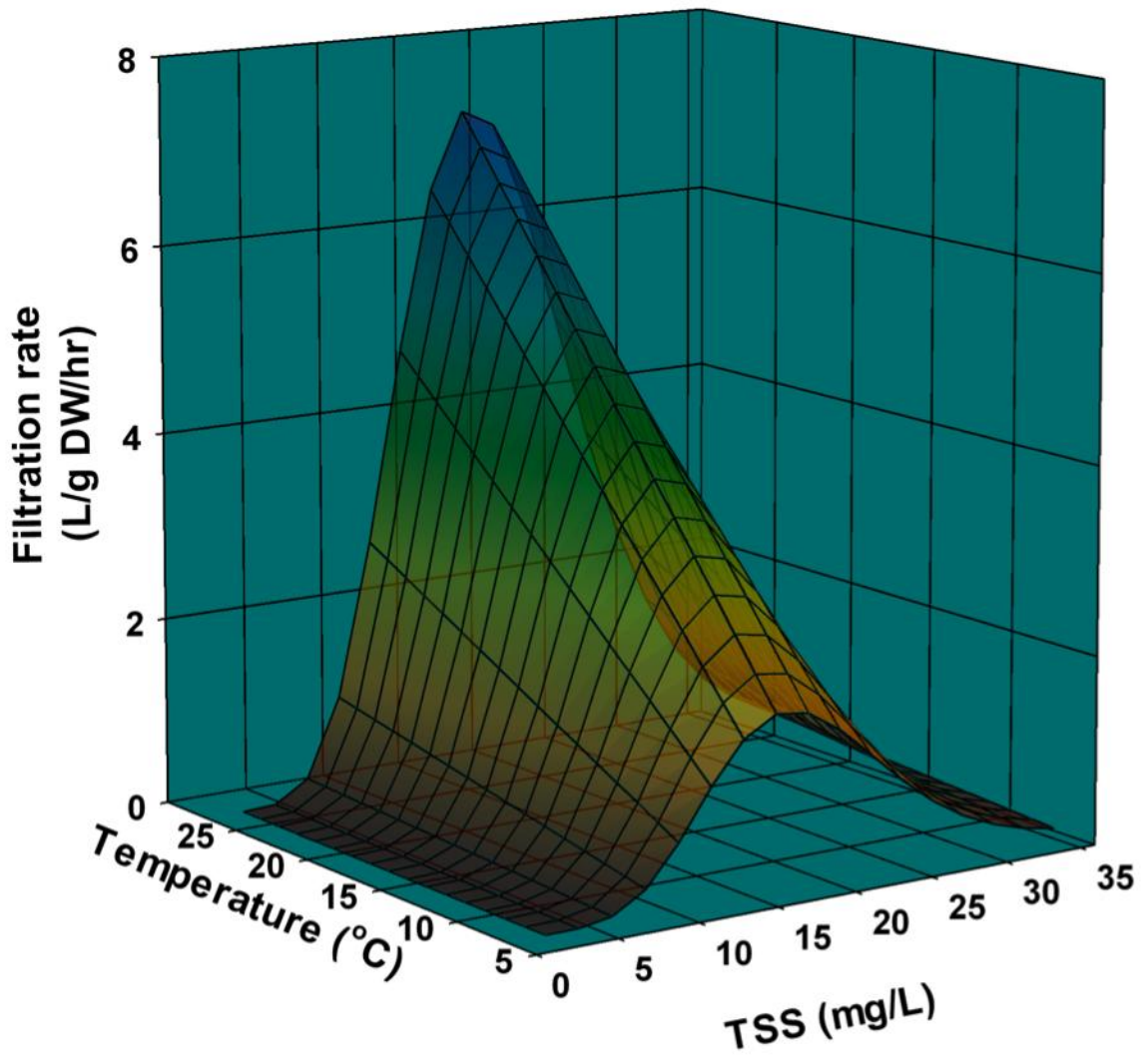
Figure III.28. Mesh plot of the function relating filtration rate to seston concentration and water temperature.

CHAPTER IV. SUMMARY AND CONCLUSIONS

Through their filtration activity, oysters remove phytoplankton, sediments, and other suspended particles from the water column. The fate of these materials and the associated nutrients depends upon physical, chemical and biological factors in the environment. Sediments deposited on the bottom may be resuspended, temporarily buried, or incorporated more deeply into the reef matrix, resulting in longer-term burial. A portion of the ingested nutrients become incorporated into the soft tissues and shell of the oyster. If the oyster is subsequently harvested, these nutrients will be removed from the water body. If the oyster is not removed from the water, then the nutrients within the soft tissue are eventually recycled through the system when the oyster dies. Nutrients sequestered within the shell matrix are effectively removed from the water body for a longer period of time. A portion of the nitrogen ingested by oysters is excreted directly back into the water column in the form of ammonium (NH_4^+) where it is available for uptake by phytoplankton and macroalgae. Finally, oyster biodeposits (feces and pseudofeces) contain organic nitrogen and phosphorus. Once on the bottom, phosphorus dynamics are heavily influenced by sediment chemistry and in general are poorly characterized. Nitrogen dynamics are also complex and largely driven by microbial activity. Through a series of processes termed *nitrification* organic nitrogen is transformed via the action of aerobic microbes to NH_4^+, NO_2 and NO_3, all of which may be released from the sediments and support the growth of benthic microalgae and macroalgae and phytoplankton (see Fig. I.1). Under the proper conditions a portion of the NO_2 and NO_3 may be converted by anaerobic bacteria to N_2 gas that escapes from the water column into the atmosphere.

This study represents a first attempt to quantify the fate of some of these materials, primarily nutrients, as they cycle through oyster reefs in the Lynnhaven River. Fully quantifying the fate of materials processed by oyster throughout the Lynnhaven will require long-term seasonal rate measurements across a wide range of environmental conditions coupled with dynamic water quality modeling. Though this scale of effort was beyond the scope of this project, our findings reveal much about the effects of oyster reefs in the Lynnhaven River on the fate of nutrients, especially nitrogen, within the system.

The sites for which we characterized nutrient dynamics in the Lynnhaven River vary in oyster abundance, oyster biomass, substratum characteristics, and tidal emersion. At the intertidal sites located at Humes Marsh, we observed strong, linear relationships between oyster biomass in the field and O_2, NH_4^+, and NO_{2+3} fluxes in the incubation chambers. We observed similar relationships between these fluxes and total faunal biomass in the incubation chambers, but only when shell biomass from living oysters was included in the calculation. Two of the Long Creek stations (1F2F and LCW) also fit this pattern of strong relationships between biomass and fluxes of O_2, NH_4^+, and NO_{2+3}. The One Fish-Two Fish site is intertidal, sandy-mud bottom with a low density of oysters, while the Long Creek West site is a subtidal, sandy-mud bottom with a low density of oysters. The one site that was consistently an outlier in these relationships was LCE, a subtidal site with a shell base bottom and a low density of oysters. We discuss possible reasons for the divergent responses at this site later in this section.

Denitrification rates (measured as rates of N_2 production) were not as tightly coupled to oyster biomass as with oxygen uptake, ammonium production or nitrite and nitrate production. At the Humes Marsh sites there appeared to be a threshold response in denitrification rates between the HMLsed and HML sites. These sites differed in two apparent ways: the presence of a thick shell base and a modestly greater oyster density at HML compared to HMLsed. Though high variation between replicate quadrats resulted in lack of statistical significance in our estimated mean oyster densities between these two field sites, we suspect that actual densities do vary between the sites and, more importantly, there were differences in the abundance and biomass of oysters from these two field sites in the chambers used to measure the fluxes (see Tables III.2 and III.3). Whether the response is due to the presence of a shell base or oyster densities above a threshold (somewhere between 50 and 120 oysters m^{-2}) the result at Humes Marsh is that all of the reefs with a shell base have comparable N_2 fluxes (Fig. III.13). At the Long Creek sites, we again observed that 1F2F and LCW sites generally fit the pattern observed at Humes Marsh sites (Fig. III.13) and that an asymptotic relationship appears to exist between oyster density and N_2 flux above about 60 g m^{-2}. The Long Creek East site was again an outlier in this relationship.

If we exclude the LCE site from the analyses, we observe a very good relationship between total nitrogen flux and oyster soft-tissue biomass at our field sites (Fig. IV.1). This suggests that, via their filtration, oysters play a prominent role in the delivery of organic nitrogen to the bottom at these sites.
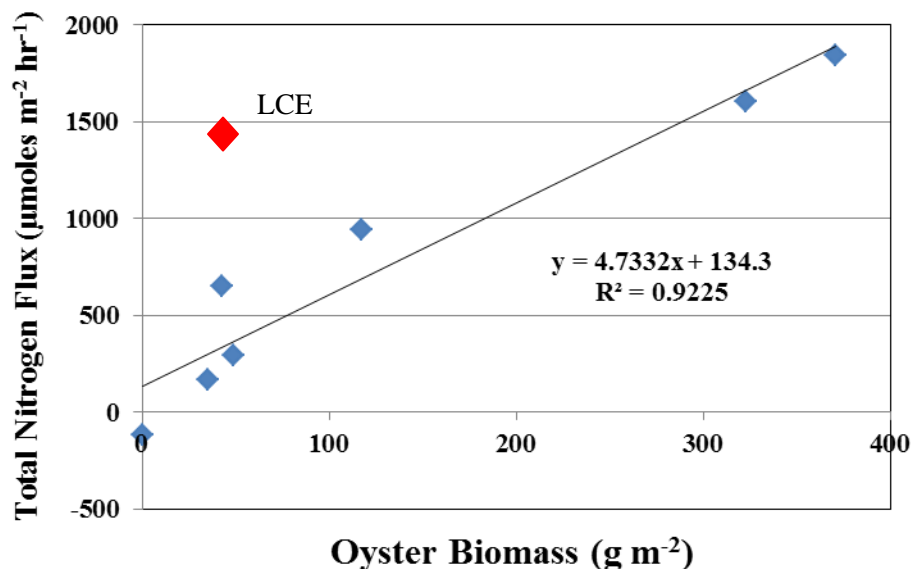
Figure IV.1. Total nitrogen flux as a function of oyster soft-tissue biomass at each of the field sites. Regression line is calculated excluding data from LCE.

Once on the bottom, much of this nitrogen is released back into the water column as NH_4^+ and is available to phytoplankton, benthic microalgae and macroalgae. At the sites in our study that had live oysters (exclusive of LCE), an average of 21% (range 11.4 – 40.4%) of the organic nitrogen underwent nitrification, yielding NO_2 and NO_3, and an average of 12%

(range 0 – 28.7%) underwent denitrification, yielding N_2. The portion of the NO_{2+3} that did not undergo denitrification was available for uptake by algae.

Two factors appear to be driving the divergent nitrogen flux patterns observed at LCE. First, the delivery of organic nitrogen to the benthos at this site appears to be driven by factors other than oyster filtration, since we observe relatively high fluxes of inorganic N out of the sediment at low oyster densities (Fig. IV.1). Second, high rates of nitrification (78.5% of total nitrogen flux) coupled with only modest rates of denitrification (19.8% of total nitrogen flux) (Fig. III.19) lead to higher rates of NO_{2+3} flux than were observed at the other sites (see Figs. III.10, III.17, and III.18). We do not know, however, what process is responsible for the delivery of excess organic matter to the bottom at this site, nor do we know why the nitrification rates are so much higher at this site. For this reason, we have excluded the LCE site in our summary computations below.

The biological processes (e.g. phytoplankton growth, oyster filtration, and microbial growth rates) that affect nitrogen cycling are strongly temperature-dependent. Thus, the rates that we report here are reflective only of the season and conditions under which they were measured. Our chamber base trays were deployed in the field for 33-34 days in September and October 2011; we thus expect that the organic nutrient loading and the micro-, meio- and macro-benthic communities are reflective of that period only. The flux rates that we measured in the incubation chambers also reflect the temperature and salinity conditions on the day that the incubations were run. It is important, therefore, that we exercise caution in extending our results beyond the conditions under which they were collected. In Table IV.1 we extend our flux estimates from the units of μmoles of N m^{-2} hr^{-1} to lbs N $acre^{-1}$ $month^{-1}$ for each station (exclusive of LCE). The first section of this table reports the amount of N that would potentially be recycled within the water column and the second section the amount that would potentially be removed from the system by a one-acre reef over a 30-day period in the fall. It is important to note that, in addition to assuming that rates are constant throughout the 30-day period and across an entire acre of substratum, these calculations assume that fluxes remain the same when substrates are exposed to air at low tide, an assumption that likely results in significant overestimates of actual rates. The final section of the table reports the amount of N sequestered in the soft-tissues and shells of macrofauna. Nitrogen sequestration is reported as a standing stock and not a rate because we lack information about the rate of growth and reproduction of the organisms involved.

The incorporation of the findings of this investigation into the Lynnhaven River water quality model can serve to alleviate the dilemma of not being able to extend these measurements throughout all portions of the Lynnhaven that are suitable for the construction of oyster reefs. One key issue here is how the impacts of oyster reefs on water quality vary temporally and spatially. The variations over temporal scales include the seasonal differences such as those shown by Kellogg et al. (2011) for the Choptank River, MD reefs for which nitrogen fluxes showed progressive increases from November to April, April to June, and June to August. Other variations over temporal time scales include the intratidal effects of those oyster reefs that are exposed over a portion of the low tide cycle. During this period of oyster reef exposure, there is no removal of nutrients and suspended sediments from the water column. Variations over spatial scales result primarily from variations in the geometry for shallow

water regions such as the Lynnhaven. The suitability for optimal growth from oyster reefs is dependent on factors such as local bathymetry as well as water quality conditions.

Table IV.1. Summary estimates of nitrogen fluxes and sequestration by site. See text for discussion of methods used to calculate monthly rates and constraints on their proper use.

	Site							
	HM0	**HMLsed**	**HML**	**HMM**	**HMH**	**1F2F**	**LCW**	**LCE**
Nitrogen recycling rates $NH_4^+ + NO_{2+3}$ flux								
μmoles m^{-2} hr^{-1}	-131.81	141.71	774.99	1482.46	1620.06	539.07	139.07	1148.33
lbs acre^{-1} month^{-1}	-11.83	12.72	69.55	133.04	145.39	48.38	12.48	103.05
Nitrogen removal via denitrification								
μmoles m^{-2} hr^{-1}	11.47	25.28	168.59	123.44	225.15	108.46	153.79	319.59
lbs acre^{-1} month^{-1}	1.03	2.27	15.13	11.08	20.21	9.73	13.80	28.68
Nitrogen removal via sequestration								
g m^{-2}	3.66	12.04	73.70	71.46	55.66	30.60	59.19	7.00
lbs acre^{-1}	32.6	107.25	656.48	635.53	495.79	272.57	527.23	62.45

The goal of this study was to provide estimates of (1) oyster filtration rates, (2) biodeposition rates, (3) nutrient flux rates between the sediment and water column, and (4) nutrient sequestration in relation to oyster biomass on reefs in the Lynnhaven River, with the intent that these would then be incorporated in the future into the water quality model to predict system-wide effects of oysters on water quality.

The regression equation in Figure IV.1 provides a basis for estimating total nitrogen flux during the early fall in relation to oyster biomass in the Lynnhaven system. Though further research is needed to clarify the factors leading to varying rates of nitrification and denitrification observed in this system, we recommend in the meantime that the water quality model employ the observed mean values of 21% and 12% of total nitrogen flux in computing nitrification and denitrification rates, respectively, during the fall. Extending the estimates of nitrogen flux from this study to annual rates will require quantification of these rates in other seasons. Based on our observations at LCE, we also recommend additional study of subtidal oyster reefs on shelly bottom to determine whether the divergent rates we observed at LCE are typical of this type of environment.

While we believe that estimating annual denitrification rates based on our data from a single season would be premature, we can place our results in context by comparing them to two other studies of oyster reef denitrification that did collect data seasonally. Piehler and Smyth (2011) collected sediment cores from within an intertidal oyster reef in North Carolina in February (11.32°C), May (14.95°C), July (29.45°C) and October (24.02°C) and report average denitrification rates of ~30, 60, 190 and 80 μmoles m^{-2} hr^{-1}, respectively. While our measurements are fairly similar to those reported by Piehler and Smyth (2011), rates measured at seven of our eight stations are higher than their October values despite the lower

temperatures at our sites. At present, it is not possible to determine whether the differences in measured denitrification rates between these systems represent actual differences between these two locations or result from methodological differences between the two studies. In contrast, studies by Kellogg et al. (2011) used methods almost identical to those in the present study, but found much higher rates of denitrification for subtidal reefs in the Choptank River, MD. The total macrofauna (including oysters) biomass density at the HMH and HMM incubation chambers in the present study (14.18 and 13.25 kg m^{-2}, respectively) was 73-78% of that from the restored oyster reef site (18.03 kg m^{-2}) in Kellogg et al. (2011). Using Choptank data from August and November to create a regression of denitrification rate to temperature, we estimate that the denitrification rate on the Choptank reef at 20°C in the fall is 923.6 μmoles m^{-2} hr^{-1}. The average of our measured denitrification rates at HMH and HMM stations was 174.30 μmoles m^{-2} hr^{-1}, suggesting that denitrification rates at this site in the Lynnhaven were approximately 19% of those observed in the Choptank. Assuming it is appropriate to use this percentage and the annual rate calculated for the restored reef in the Choptank to get a first-order estimate of annual denitrification rates at HMH and HMM, we estimate that annual denitrification rates at these two stations could be as high as 103 lbs N acre^{-1} yr^{-1}. However, this simplified estimate does not take into account several factors that should be part of any future modeling efforts, most obviously tidal cycles and length of day. Because the results of the present study do not demonstrate a strong linear relationship between denitrification rates and any of the site characteristics we measured, we do not currently have sufficient data to make even first-order estimates of annual denitrification rates for our other six field sites.

The nutrient recycling differences between Choptank River oyster restoration sites and the shallow water sites in this study are large, reflecting a number of site differences. The Choptank site is ~7 m deep, with the likelihood of resuspension and removal of oyster biodeposits much lower than likely found at the Lynnhaven site. Moreover, despite similar oyster biomass, the expected higher phytoplankton biomass in the highly eutrophic Choptank River may lead to greater production of pseudofeces. The similar stochiometry of oxygen and ΣN at these sites suggest that the main difference is in the supply of organic matter to the reef community, rather than a large shift in the efficiency of microbial processes. The average efficiency of denitrification is somewhat higher in the Choptank River, possibly reflecting a greater efficiency of nitrification, possibly from an increased residence time of water within the oyster matrix. The influence of physics on denitrification efficiency of oyster communities remains unknown, but is likely to be a key determinant in the water quality value of restored reefs.

Our findings do not suggest that oyster reefs play a very significant role in phosphorus dynamics in the Lynnhaven River. Estimates of phosphorus sequestration on reefs with shell bases in our study ranged from 1.9 – 11.3 g m^{-2} (Table III.6), but these represent only single point in time estimates and not a rate of phosphorus uptake. Fluxes of soluble reactive phosphorus between the bottom and the water column were low and not clearly related to oysters in our study (Fig. III.21). We observed phosphorus release at only two stations (HMM and HMH) and then only under light conditions. At all other stations with oysters phosphorus was removed from the water column (Fig. III.21).

With regard to biofiltration and biodeposition, the first element of this section involved calculation of the relationship between Oyster Mass (ash-free dry mass, AFDM) in g and Shell Height (SH) in mm specifically for the Lynnhaven River system. This function was exponential and can be used as a standard for comparison with studies in other locations to generate the expected weight of oysters of different sizes when determining biomass-specific filtration and biodeposition rates. Next we analyzed the relationship between Biodeposition Rate and Total Suspended Solids (TSS), as derived from the Jordan (1987) data set. Examination of the diagnostic measures for this analysis indicated that there were serious deviations from the statistical assumptions underlying regression analysis. Given the poor fit of the biodeposition data in the previous analysis, we analyzed the Biodeposition data as a function of Seston concentration and Water Temperature with non-linear regression. For biodeposition (and thus filtration), the relationship between Biodeposition Rate and Seston concentration was a Ricker function with strong density dependence (Allee effect) at low TSS values. This indicates that at very low levels of seston concentration, oysters cease filtering, most likely due to the poor benefit:cost metabolic ratio at low seston concentrations. Specifically, oysters will expend more energy filter feeding at low seston concentrations than they receive from the filtered material. In contrast, at high seston concentrations biodeposition rates were low due to an inability of oysters to filter effectively at high seston concentrations, such that their filtration apparatus becomes clogged with sediment particles and shuts down. Next we modeled biodeposition rate as a joint function of the two independent variables (seston concentration and water temperature). Finally, we used the preceding model to generate an equation relating filtration rate as a function of seston concentration and water temperature. Moreover, biodeposition and biofiltration are positively related to oyster weight, such that water quality measures need not account for oyster reef height, but only oyster biomass as determined from oyster reef and habitat surveys.

The findings of this study provide a starting point towards our ultimate goal of providing state and local government officials with a more complete understanding of the role that oyster reefs can play in meeting water quality improvement standards. Whether through actions related to conservation of existing reefs or active restoration of oyster reefs, it is clear that enhancing oyster populations has the potential to remove substantial quantities of suspended sediment and nutrients from the water column. Our first-order estimate of 103 lbs. of N acre^{-1} yr^{-1} removed as a result of denitrification associated with oyster reefs needs to be improved using seasonal measurements and static sequestration values need to be converted to rates of nutrient sequestration based upon annual growth and survival rates of oysters and reef-associated macrofauna. Once validated these rates could then be used either to refine the water quality model used to set loading targets for a water body or to establish the value of constructed oyster reefs as a BMP for reducing loadings.

V. LITERATURE CITED

Ambrose RB, Vandergrift SB, Wool A (1986) WASP3, a Hydrodynamic and Water Quality Model- Model Theory, *User's Manual, and Programmers Guide*. Report No. EPA/6000/3-86-034. USEPA Environmental Research Lab. Athens, Ga.

Berg P, Roy H, Janssen F, Meyer V, Jorgensen BB, Huettel M, de Beer D (2003) Oxygen uptake by aquatic sediments measured with a novel non-invasive eddy correlation technique. Mar. Ecol. Prog. Ser. 261: 75-83.

Boynton WR (2000) Impact of nutrient inflows on Chesapeake Bay. In: Sharpley AN (ed) Agriculture and Phosphorus Management: The Chesapeake Bay. Lewis Publishers, Boca Raton.

Boynton WR, Bailey EM (2008) Sediment Oxygen and Nutrient Exchange Measurements from Chesapeake Bay, Tributary Rivers and Maryland Coastal Bays: Development of a Comprehensive Database & Analysis of Factors Controlling Patterns and Magnitude of Sediment-Water Exchanges. UMCES Technical Report Series No. TS-542-08. University of Maryland Center for Environmental Science.

Boynton WR, Hagy JD, Cornwell JC, Kemp WM, Greene SM, Owens MS, Baker JE, Larsen RK (2008) Nutrient budgets and management actions in the Patuxent River estuary, Maryland. Estuaries and Coasts 31:623-651

Boynton WR, Kemp WM (1985) Nutrient regeneration and oxygen consumption by sediments along an estuarine salinity gradient. Marine Ecology Progress Series 23:45-55

Burke RP (2010) Alternative Substrates are Effective in Native Oyster (*Crassostrea virginica*) Reef Restoration in Chesapeake Bay. PhD dissertation, The College of William & Mary

Cerco CF, Cole T (1995) *User's Guide to the CE-QUAL-ICM Three-Dimensional Eutrophication Model.* Technical Report EL-95-15, U.S. Army Engineer Waterways Experiment Station, Vicksburg, MS, 316.

Cerco CF, Nole MR (2007) Can oyster restoration reverse cultural eutrophication in Chesapeake Bay? Estuaries and Coasts 19:562-580.

Chick, CR (2009) Benthic oxygen production in the Choptank estuary. M.S. Thesis, MEES Program. University of Maryland – College Park. 71p.

Cornwell JC, Kemp WM, Kana TM (1999) Denitrification in coastal ecosystems: environmental controls and aspects of spatial and temporal scale. Aquatic Ecology, 33:41-54.

Cowan JLW, Boynton WR (1996) Sediment-water oxygen and nutrient exchanges along the longitudinal axis of Chesapeake Bay: Seasonal patterns, controlling factors and ecological significance. Estuaries 19:562-580

Dame RF, Spurrier JD, Wolaver TG (1989) Carbon, nitrogen and phosphorus processing by an oyster reef. Marine Ecology Progress Series 54:249-256

Dame RF, Zingmark R, Stevenson LH, Nelson D (1980) Filter feeder coupling between estuatrine water column and benthic subsystems. Pp. 521-551, In: Kennedy VC (ed) Estuarine perspectives, Academic Press, New York

DeAlteris JT (1988) The Geomorphic Development of Wreck Shoal, a Subtidal Oyster Reef of the James River, Virginia. *Estuaries* 11:240-249

Grizzle R, Ward K (2011) Experimental quantification of nutrient bioextraction potential of oysters in estuarine waters of New Hampshire. Final Report to The Piscataqua Region Estuaries Partnership, Durham, NH

Hammond DE, Cummins KM, McManus J, Berelson WM, Smith G, Spagnoli F (2004) Methods for measuring benthic nutrient flux on the California Margin: Comparing shipboard core incubations to in situ lander results. Limnology and Oceanography Methods 2:146-159

Haven, DS, Morales-Alamo R (1972) Biodeposition as a factor in sedimentation of fine suspended solids in estuaries, p. 121-130. In: *Geol. Soc. of Am. Memoir* No. 133. Geological Society of America, New York.

Higgins CB, Stephenson K, Brown BL (2011) Nutrient Bioassimilation Capacity of Aquacultured Oysters: Quantification of an Ecosystem Service. Journal of Environment Quality 40:271

Holyoke RR (2008) Biodeposition and biogeochemical processes in shallow, mesohaline sediment of Chesapeake Bay. Ph.D., UMCP, College Park

Jordan S (1987) Sedimentation and remineralization associated with biodeposition by the American oyster *Crassostrea virginica* (Gmelin). PhD dissertation, University of Maryland, College Park

Kana TM, Darkangelo C, Hunt MD, Oldham JB, Bennett GE, Cornwell JC (1994) Membrane inlet mass spectrometer for rapid high-precision determination of N_2, O_2, and Ar in environmental water samples. Analytical Chemistry 66:4166-4170

Kellogg, ML, Cornwell, JC, Paynter, KT, Owens MS (2011) Nitrogen removal and sequestration capacity of a restored oyster reef: Cheasapeake Bay experimental studies. Final Report to the Oyster Recovery Partnership, Annapolis, MD. UMCES Technical Report Series TS-623-11. 65 pp.

Kirby, MX, TM Soniat, Spero HJ (1998) Stable Isotope Sclerochronology of Pleistocene and Recent Oyster Shells (Crassostrea virginica). Palaios 13:560-569

Miller-Way T, Boland GS, Rowe GT, Twilley RR (1994) Sediment oxygen consumption and benthic nutrient fluxes on the Louisiana continental shelf: A methodological comparison. Estuaries 17:809-815

Newell, RIE 1988. Ecological Changes in Chesapeake Bay: Are they the result of overharvesting the American oyster (Crassostrea virginica), p. 536-546. In M. Lynch (ed.), Under-standing the Estuary: Advances in Chesapeake Bay Research. Chesapeake Research Consortium Publication 129, Glouces-ter Point, Virginia.

Newell R, Fisher TR, Holyoke R, Cornwell J (2005) Influence of eastern oysters on nitrogen and phosphorus regeneration in Chesapeake Bay, USA. In: R Dame, S Olenin (eds) The Comparative Roles of Suspension-Feeders in Ecosystems. Kluwer, Netherlands

Newell RIE (2004) Ecosystem influence of natural and cultivated populations of suspension-feeding bivalve molluscs: areview. Journal of Shellfish Research 23: 51-61.

Newell RIE, Koch EM (2004) Modeling seagrass density and distribution in response to changes in turbidity stemming from bivalve filtration and seagrass sediment stabilization. Estuaries 27: 793-806.

Newell RIE, Owens MS, Cornwell JC (2002) Influence of simulated bivalve biodeposition and microphytobenthos on sediment nitrogen dynamics. Limnology Oceanography 47:1367-1369

Parsons TR, Maita Y, Lalli CM (1984) A Manual of Chemical and Biological Methods for Seawater Analysis, Pergamon Press, New York

Piehler MF, Smyth AR (2011) Habitat-specific distinctions in estuarine denitrification affect both ecosystem function and services. Ecosphere 2:1-16

Powell, EN, Kraeuter JN, and Ashton-Alcox KA (2006) How long does oyster shell last on an oyster reef? Estuar. Coast. Shelf Sci. 69:531-542

Reay, W. G., D. L. Gallagher, and G. M. Simmons, Jr. 1995. Sediment-water column oxygen and nutrient fluxes in nearshore in environments of the Delmarva Peninsula, USA. Marine Ecology Progress Series **118:** 215-227.

Sisson M, Wang H, Li Y, Shen J, Kuo A, Gong W, Brush M, Moore K (2010a) "Development of Hydrodynamic and Water Quality Models for the Lynnhaven River System." Final Report to the U.S. Army Corps of Engineers, Norfolk District and the City of Virginia Beach. Virginia Institute of Marine Science. Special Report No. 408 in Applied Marine Science and Ocean Engineering. 205 pp.

Sisson M, Li Y, Wang H, Kuo A (2010b) "Numerical Modeling Scenario Runs to Assess TSS and Chlorophyll Reductions Caused by Ecosystem Restoration, Lynnhaven River " Final Report to the U.S. Army Corps of Engineers, Norfolk District and the City of Virginia Beach. Virginia Institute of Marine Science. Special Report No. 422 in Applied Marine Science and Ocean Engineering. 41 pp. & Appendix.